X-713-65-468

NASA TM X-55399

THERMAL ANNEALING OF RADIATION DAMAGE IN SOLAR CELLS

BY

P. H. FANG

NOVEMBER 1965

GODDARD SPACE FLIGHT CENTER

GREENBELT, MARYLAND

X-713-65-468

THERMAL ANNEALING OF RADIATION DAMAGE IN SOLAR CELLS

by

P. H. Fang
Thermal Systems Branch
Spacecraft Technology Division

November 1965

GODDARD SPACE FLIGHT CENTER
Greenbelt, Maryland

CONTENTS

LIST OF FIGURES

THERMAL ANNEALING OF RADIATION DAMAGE IN SOLAR CELLS

I. INTRODUCTION

Silicon solar cells have been used as the electric power sources since the first Vanguard satellite, and it appears that this type of cell will be the principal power source for some time to come. One problem in using the silicon solar cell for a long duration is its vulnerability to space radiation (Reference 1). At present, four different approaches are being developed to minimize this radiation damage problem in silicon solar cells: These are

1. Drift field solar cells;
2. Silicon solar cells with different doping impurities,
3. Cells which provide for compensation of radiation damage by mobile impurities, such as Lithium; and
4. Methods for thermal annealing of radiation damage.

These methods are listed in a chronological order, however, the last two, which were started almost simultaneously, after the 1964 International Conference on Radiation Damage, held at Royaumont, France.

1. In the drift field approach, the drift field is produced by a concentration

gradient which is introduced in the base (p-type region) so that minority carriers whose life times were reduced by radiation damage might still reach the np junction with the aid of the drift field (Reference 2). This approach has been carried out since 1962 by Electro Optical Systems, Inc. (Reference 3). But a more systematic approach with a more realistic model has been undertaken within the last six months particularly at Heliotek, Texas Instruments, Inc., Electro Optical Systems, Inc. (Reference 4), and Goddard (Reference 5). The success of this approach is yet to be seen.

2. The experiment with different impurities is interesting because the capture or recombination cross-section is expected to depend on the impurities (Reference 6). However, very little experimental work has been done on this fundamental problem. In the meantime, some success in diminishing the amount of radiation damage in the solar cell by using Al as the p-type impurity has been reported by J. Mandelkorn (Reference 7). The result was not universally accepted because of the difficulty in reproducing the result in other laboratories, and because of the complexities in the technology of solar cell production.

3. Because of the unusually high solubility of the Lithium ion, even at room temperature, and the small ionization energy of Lithium, the possibility of interaction between the Lithium impurity and the radiation produced defects has been investigated, principally, by V. S. Vavilov (Reference 8). Since late 1964, experiments on Lithium diffusion were carried out both with surface barrier diodes and

solar cells, at RCA Princeton Laboratories and RCA Mountain Top Laboratories (Reference 9). No definite evidence of lessening radiation damage has been established at this early stage.

4. Thermal annealing of radiation damage in silicon was known in the early history of radiation damage studies. In a paper of Bemski and Augustyniak in 1957, annealing of electron damage in silicon was reported (Reference 10). They considered the defects to be vacancies and interstitials; today we know the defects that are stable even above liquid nitrogen temperature are those associated with impurities. They believed that the distribution of these defects is uniform and that there is no cluster effect. In the present work, we shall prove that this is not the case. They used a mathematical model of annealing kinetics which is oversimplified in the light of present advances. However, the remarkable result was that they found, for the first time, that damage can be annealed in the temperature range of 300 to 400°C, and that the exact annealing temperature is related to the annealing time by an activation energy of 1.3 ev. These results have since been substantiated by other investigations.

Basic work on annealing has become available gradually during the last three years, principally through the works of Pell (Reference 11), Watkins (Reference 12), J. Corelli (Reference 13), and Stein (Reference 14). A very useful paper is that of Hasiguti and Ishino (Reference 15). This reference provides a sufficient foundation for investigating the feasibility of thermal annealing in

technically important devices such as solar cells and transistors. It was an opportune moment when I contacted Professor Hasiguti in July, 1964. At that time RCA Mountain Top Laboratories, who were to provide most of the solar cells for our subsequent experiments had changed the electrode contact from a solder dip, which was stable only below 200°C to an evaporated electrode of Ag-Ti alloy (which can be heated to 600°C, well above 400°C where the important annealing occurred). I would like to record here my pleasant experience in the discussion with Professor Hasiguti and the accommodating help of Mr. A. Topper of RCA Mountain Top Laboratories.

The result of our experiments have been so successful that at the end of this report we shall venture to discuss a scheme for applying the results obtained in this work to space power systems (Reference 16).

The work reported here is by no means complete. However, the results we have obtained thus far are sufficient to encourage those who have the forthright vision to contemplate future applications. For this purpose, early dissemination of the information is essential, while there is no doubt that much work has yet to be done to optimize the present findings for utilization.

This report is addressed primarily to experimenters who are interested in using the present results for practical applications. Therefore, I have referred to all the necessary literature, but have not attempted to cover completely the physics of annealing.

I would like to acknowledge the important help of Messrs. Y. M. Liu and G. Meszaros with the experimental work, also of Mr. W. Gdula for an early brief period. I would like to thank my Branch Chief, Mr. M. Schach who has shown great understanding and friendly encouragement. Prompt recognition of the work in the early stage by our Division Chief, Mr. W. Matthews, provided much of the impetus for this investigation. Finally, I would like to acknowledge the helpful comments of my colleagues of the Radiation Physics Group. Many experimental problems and interpretations are the results of discussions and deliberations in our frequent seminars.

REFERENCES

1. See annual Photovoltaic Specialist Conference, 1963, 1964 and 1965, published by Power Information Center, University of Pennsylvania, Philadelphia, Pa.
2. Wolf, M., Proc. IEEE 51, 674 (1963).
3. Contract NAS7-92, February 1963.
4. Contract NAS5-3588 with Heliotek (completed since December 1964). Contract NAS5-9609 with Texas Instr. (continuing), Contract NAS5-9612 with EOS (continuing).
5. Fang, P.H., Proc. 4th Photovoltaic Specialist Conference, V. 1, B 1 (1964).

6. Lax, M., Phys. Rev. 119, 1502 (1960).

7. Mandelkorn, J., Photovoltaic Specialist Conference, V. 1, A 6 (1964), J. Appl. Phys. 35, 2258 (1964).

8. Vavilov, V.S., L.S. Smirnov and V.A. Chapnin, Soviet Phys. Solid State (Transl.) 4, 2467 (1963, J. Phys. Soc. Japan 18, Suppl. 3, 236 (1963).

9. Contract NAS5-3788 and NAS5-3686 respectively.

10. Bemski, G. and W.M. Augustyniak, Phys. Rev. 108, 645 (1957).

11. Pell, E.M., J. Appl. Phys. 32, 1048 (1961), Phys. Rev. 119, 1222 (1960).

12. Watkins, G., 7^{e} Congres International Effects des Rayonnements sur les Semiconducteurs, Paris 1964 (Dunod 1965) p. 97.

13. Corelli, J.C., G. Oehler, J.F. Becker and K.J. Eisentraunt, J. Appl. Phys. 36, 1787 (1965), J.C. Corelli and L.J. Chen (to be published).

14. Stein, H., Sandia Report, 1964

15. Hasiguti, R.R. and S. Ishino, op. cit. ref. 12, p. 259.

16. Fang, P.H., W. Gdula and G. Meszaros, NASA Patent Application.

II. THERMAL ANNEALING OF RADIATION DAMAGE

In contrast to the considerable amount of knowledge available on the annealing of defects in metals (Reference 1), our knowledge in the case of semiconductors is much less complete. At very low temperatures, i.e. in the liquid helium temperature region, the primary defects for both metals and semiconductors are interstitials and vacancies. A basic difference between the defects in metals and semiconductors occurs at high temperature, i.e. at liquid nitrogen temperature and above, while interstitials and vacancies remain as stable defects in metals, in semiconductors defects are no longer stable and can be readily annealed. The defects in semiconductors which are stable at high temperatures are complex: namely associations between interstitials and vacancies among themselves or with impurities. This basic distinction cannot be stressed enough. One good example is the early result of annealing of Silicon and Germanium by Bemski and Augustyniak (Reference 2). They did an experiment correctly, but interpreted their results incorrectly by treating the defects like those found in metals. Today many references can still be found in the literature about their pioneer work, but one should not consider their explanations too seriously.

The basic understanding of the thermal annealing in terms of specific types of defects is a very recent event. Two review articles give summaries of our present knowledge (References 3 and 4). While the details of the different types of defect structures can be found in Reference 3, we reproduce in Figure II-1

an atlas of the isochronal annealing of Silicon. For practial purposes, we are interested only in the defect centers which are stable above room temperature. Figure II-1 shows 4 such stable defect centers, E, A, C, and J. There is also a reverse annealing which one observes above 150°C.

Some evidence from photoconductivity (Reference 5) and infrared absorption (Reference 3) as well as EPR (Reference 4) studies imply these are not the only stable defect centers. But even today there is not a firm understanding of the relative importance of these known defect centers for the photovoltaic effect (Reference 8). Therefore, our work and interpretation have to be limited by a phenomenological approach, carried out in a limited temperature region, between room temperature and 600°C. The lower limit is dictated by most practical applications. The high temperature limit is an intrinsic property of the unavoidable presence of oxygen in Silicon which causes the so-called thermal damage (Reference 9).

According to Figure II-1, the E center can be annealed near 200°C. The reverse annealing and A, C, J centers can be annealed near 375°C. These temperatures are sometimes referred to as the characteristic annealing temperatures. Actually they can be shifted considerably by a change of concentrations of defects, of the concentrations of impurities, and previous thermal history. The last factor seems to be of special importance in the case of solar cells. Solar cells, in the usual industrial practice, have to undergo a treatment

near 1000°C to form an n-p function by diffusion, and a consequent abrupt cooling to room temperature. According to Watkins (Reference 10), a quenching effect could shift the annealing temperature as much as 50 to 100°C. In most cases of solar cells, the annealing temperature is closer to 400°C than 350°C as found in the instances of A, C, and J center annealing of crystal silicon.

In a later discussion, we shall have occasion to show some differences in the observation of annealing according to the different methods of experiment, corresponding to use of crystals with differing types of contacts: no contact (EPR measurement), ohmic contact (Hall measurement), non-ohmic contact (surface barrier diode and transistors) and non-ohmic contact with photon injection (solar cells). We shall also have occasion to show some intrinsic scientific values, besides the practical means for using solar cells as an object for the study of annealing of defects.

We would like to claim, as far as we know, that ours is the first experiment to demonstrate the successful annealing of radiation damaged solar cells (Reference 11). We hope the knowledge derived from this report will find practical application in the space endeavor.

REFERENCES

1. Damask, A. C. and G. J. Dienes, Point Defects in Metals (Plenum Press) 1965.

2. Bemski, G. and W. Augustyniak, Phys. Rev. 108, 645 (1957).

3. Hasiguti, R. R. and S. Ishino, 7^{e} Congres International Effects des Rayonnements sur les Semiconducteurs, Paris, 1964 (Dunod 1965), p. 259.

4. Watkins, G., ibid, Ref. 3, p. 97.

5. Vavilov, V. S. and A. F. Plotnikov, J. Phys. Soc. Japan, 18, Suppl. 2, 33 (1963), ibid, Ref. 1, p.

6. Corelli, J., et al., J. Appl. Phys. 36, 1787 (1965), Phys. Rev. to appear.

8. General Atomic Report, NAS7-289 (1965), TRW Report NAS5-3805.

9. Bemski, G. and C. A. Dias, J. Appl. Phys. 35, 2983 (1964).

10. Private communications.

11. Fang, P. H., W. Gdula and G. Meszaros, NASA Patent pending.

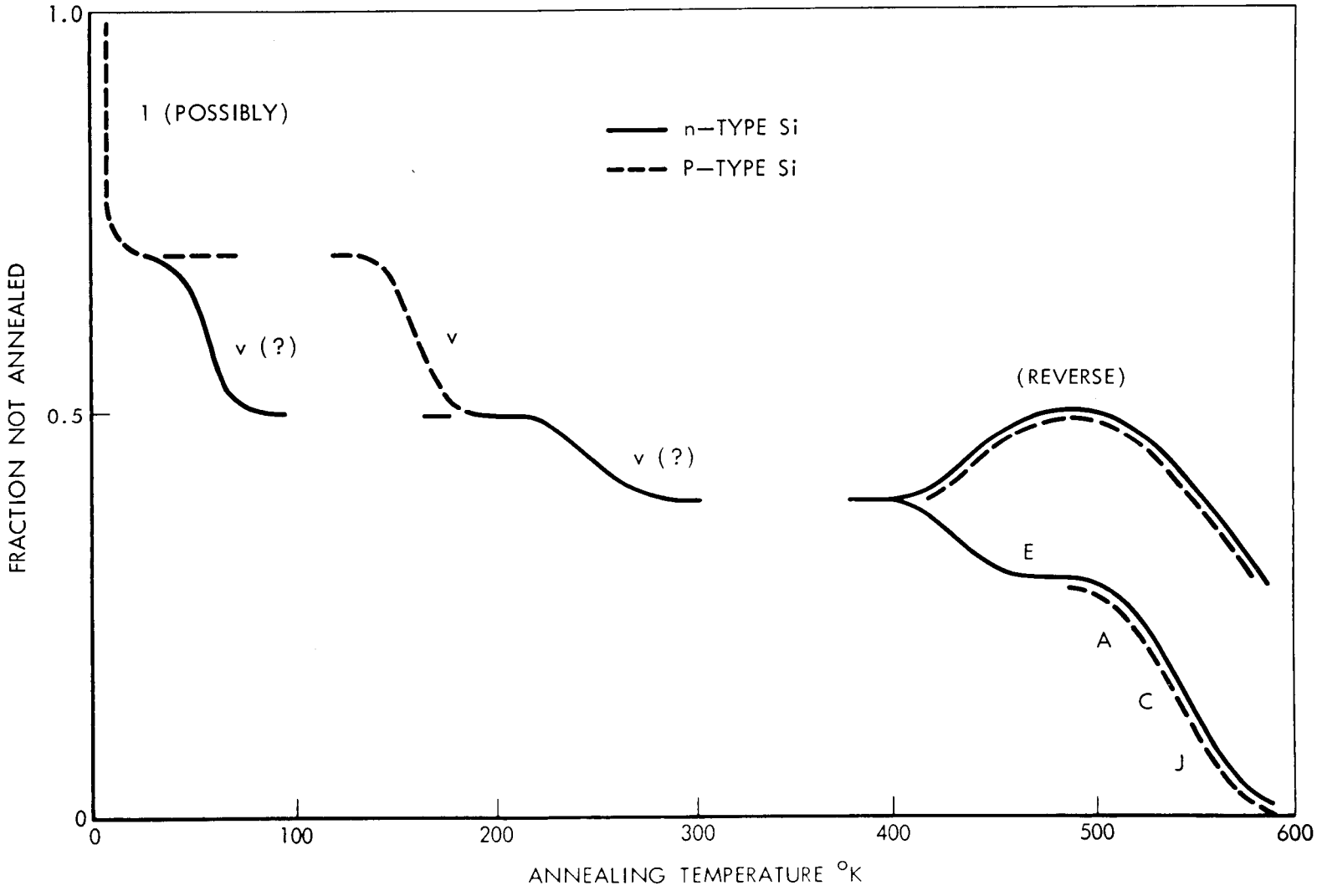

Figure II-1. Schematic Diagram of Annealing Stages in Silicon (After Hasiguti and Ishino, Reference 3)

III. EXPERIMENTAL TECHNIQUE

The solar cells were supplied by RCA Mountain Top Laboratories through Contract NAS5-9576, unless otherwise specifically mentioned. These solar cells were mostly of 10 Ω -cm base resistivity material. The silicon crystals were crucible grown, and came from different sources at different times. The specimens were from production lots and no pre-selections were made in carrying out the experiments. Our only requirement was that the cells must withstand temperature treatment up to 600°C without a change of intrinsic electrical characteristics. This fact was verified by several temperature cycling experiments.

The electron irradiation was carried out at W. Grace Company, with a 2 Mev horizontal sweeping beam about 3" wide and 18" long. The sweeping rate was 200 cps. The beam current was usually about 4 μa. In addition, copper tubing with running cold water was imbedded under the specimen holder. We observed an increase of temperature during the radiation from room temperature to less than 5°C above room temperature.

The changes in four parameters are used to measure radiation effects and annealing:

1. The short circuit current under a white light, I_S
2. The open circuit voltage under a white light, V_0
3. Spectral response of the photovoltaic current per photon of wavelength λ, or, the quantum field, Q_λ.

4. Photovoltaic current against photovoltaic voltage (IV-curve) either by injection of photons and a change of load resistivity, or use of a biased voltage. From this curve the maximum power output and the corresponding efficiency, η , is measured.

By white light we do not mean a light source with equal intensity in all spectral regions. We simply mean an artificial light source with a possible infrared cut-off filter. There is a great deal of controversy in the problem of the light source, especially in industrial practice. Currently, we are using a Xenon arc lamp with a very high output light intensity. The original idea in adopting this source was to increase the light intensity in the short wave region where the ordinary tungsten lamp does not provide a sufficient intensity. One desired improvement is a source with a spectrum closer to the solar spectrum, i.e., a solar simulator. Actually, for our purpose, it turns out that this is not essential. For many problems, we find the analysis of the spectral response parameter simpler. For our experiments, the shape of the intensity spectra is not important, provided that two factors are satisfied:

1. a linear proportionality between the light intensity and photovoltaic current exists, and
2. the superposition principle holds, i.e., there is no multichromatic effect.

For ordinary light intensities, and neglecting the very small effects at extremely short wavelengths (Reference 1), those factors are satisfied in the case of silicon

solar cells in the temperature range of interest, where the contribution from indirect band transitions is negligible.

There is an undesirable feature of Xenon arc light sources. Since the plasma stability has a very short relaxation time, a local fluctuation of the power supply or the temperature fluctuations resulting from heat or from the ozone exhaustion system cause a light intensity fluctuation of about 5%. This greatly affects the measurement of IV-curves near the short circuit condition. We are planning recourse to a simple tungsten lamp with a glass infrared filter in the near future.

Our complete experimental set up for these measurements is shown in Figure III-1 and Figure III-2. Figure III-1 shows the light source after collimation, illuminating a bank of narrow band filters. Then the light is reflected and shone on the solar cell. Electrical connections are made to record the data on an X-Y recorder for the I-V curve measurement, and to a semiautomatic system using a punch tape recorder for spectral response measurements.

We have 17 filters in the filter wheel. The wavelengths are: 3390, 3846, 4000, 4200, 4400, 5010, 5210, 5610, 6010, 6420, 6800, 7420, 8020, 8480, 9040, 9480, 10,000A. There is one empty window in the wheel which is reserved for white light entrance.

Radiation damage in this work is always a relative measurement, that is, we measure the change of the 4 parameters listed above as a function of the

radiation flux level, and in the case of annealing, as a function of isochronal annealing temperature or isothermal annealing time. Such a relative measurement does not yield directly physical quantities which can be used in the analysis of basic physical problems, but it gives a phenomenological picture and, most of all, provides data, on the basis of which practical applications can be considered.

For annealing, forming gas is introduced into the high temperature oven to avoid the oxidation of the electrodes (Figure III-2). The specimen is inserted into a platinum boat resting in the quartz tube, as shown in the figure. At this position, the specimen is less than five degrees above room temperature. When the oven reaches a desired temperature, a steel thread which is connected to the platinum boat is pulled so that the specimen will come into the annealing temperature region. Since the system is essentially closed to a draft of room temperature air, this simple arrangement can reach annealing temperature within a few seconds.

REFERENCE

1. Tuzzolino, A. J., Phys. Rev. 134, A205 (1964).

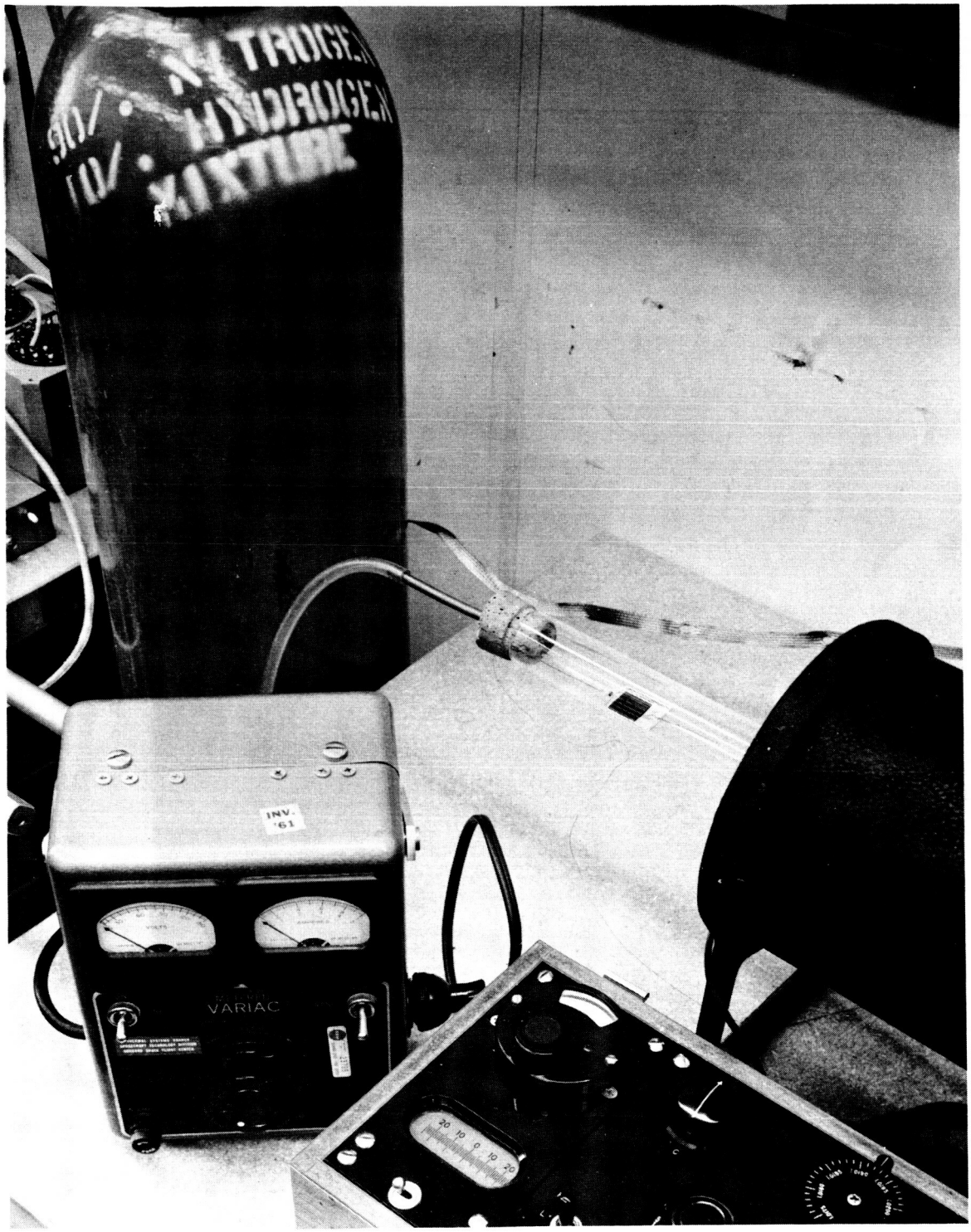

Figure III-2. Assembly for Annealing

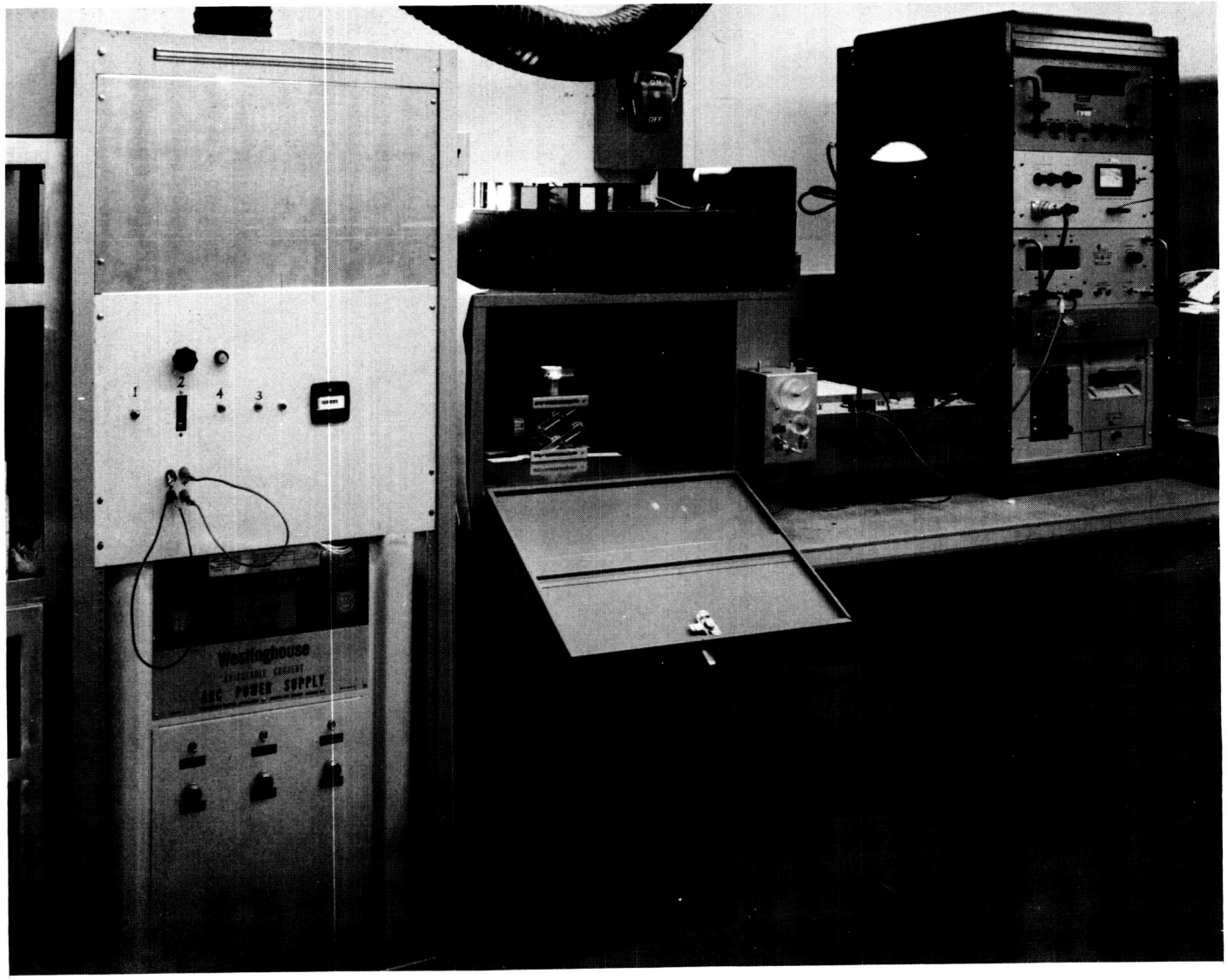

Figure III-1. Assembly for Photovoltaic Measurement

IV. ISOTHERMAL ANNEALING

In the ensuing chapters, we shall present experimental results of solar cell annealing in chronological order of the experiments. At a later time, some Addenda to individual chapters are planned when more results are obtained.

We define, first, a damage parameter, D, as

$$D_x = \left(1 - \frac{x}{x_0}\right) \cdot 100\%, \tag{1}$$

where the x's are the measured parameters, as described in Chapter III. They are, short circuit current I, open circuit voltage V, quantum field Q, and efficiency η. The notation of I will be used instead of I_S and V instead of V_0 to make the notations concise. x is measured after an irradiation, as a function of the radiation flux ϕ, or after a thermal treatment as a function of the annealing time t or of the annealing temperature T. x_0 is the value before the radiation. We emphasize here x_0 is always measured at room temperature, as is x.

Figure IV-1 is an isothermal annealing of an n on p solar cell with 10 Ω-cm base resistivity, supplied by the RCA Mountain Top Laboratories. Hereafter, unless specifically mentioned, all solar cells will be of this type. The solar cell is irradiated with 1.4×10^{14} electrons/cm^2 of 2 Mev energy. Two curves are shown, D_1 and $D\eta$. Both curves show an initial fast annealing, followed by slow leveling off and then another step which completes the annealing. These curves

resemble the curve of the original work of annealing of Bemski and Augustyniak (Reference 1). In their case, the measured parameter was the minority carrier life time.

Figure IV-2 shows a spectral response curve of a solar cell after irradiation with 4×10^{14} electrons/cm^2 of 1 Mev energy, and after a 15 minute, 400°C annealing. The results demonstrate a complete recovery, or even a slight improvement of the total quantum yield, compared to the original state of the specimen. This improvement effect is small, but by no means an exceptional case (Reference 2).

Figure IV-3 shows the dependence of the characteristics of isothermal annealing curves for three electron flux levels of 1 Mev radiation, annealed at 440°C. We observe a complete recovery for a flux level of 4×10^{14} e/cm^2 and an almost complete recovery at 8×10^{14} e/cm. For the 1×10^{15} e/cm case, the recovery is incomplete, and this effect will be discussed in detail in Chapter VI.

Figure IV-4 shows annealing carried out at 400°C, i.e., at a somewhat lower temperature from those of Figure III-3. Therefore, the annealing time is longer. The solid curve is measured under a xenon light source, and the dotted curve under a tungsten light source. The result shows that annealing is complete for $\phi = 4 \times 10^{14}$ e/cm^2. The differences in the result of $\phi = 8 \times 10^{14}$ e/cm and above are caused by incomplete annealing at different regions in the solar cells. Recovery is easier near the surface than in the bulk region (Reference 3), and

the dominance of the red light in a tungsten light source tends to exaggerate the damage in the bulk region. This is further demonstrated in Figure IV-5.

If, instead of using white light, the spectral response is measured, we obtain the results shown in Figure IV-5. Comparison between 9040A (dotted curve) and 8020A (solid curve) data for 400°C annealing shows a larger degradation and a slower approach to complete annealing in the long wavelength case. Comparison among different flux levels of radiation shows a higher effectiveness of recovery in the case of lower flux levels of radiation, or, equivalently, a lower degree of damage.

Figure IV-6 shows D_1 (solid curve) and D_V (dotted curve), for solar cells of two different base resistivities, 1 and 10 Ω-cm respectively, annealed at 375°C. The irradiation is with 5×10^{14} electrons/cm^2 at 1 Mev. The annealing of D_V is about the same for the two base resistivities, but for annealing of D_1, the one of high resistivity is better. In both cases, the annealing is quite incomplete.

Figure IV-7 shows annealing at 400°C. In this case, the annealing is more effective even with a flux level of 5×10^{15} e/cm^2. It also shows a distinct superiority of the solar cells with 10 Ω-cm base resistivity, even in annealing. The superiority of radiation resistivity of 10 Ω-cm solar cells over 1 Ω-cm solar cells has now been commonly accepted.

It will be shown in the next chapter that 5×10^{15} e/cm^2 radiation is excessive to be annealed completely. The conclusion of this chapter is that for 4×10^{14} e/cm^2 radiation, which causes about 20% damage in I_s, a complete recovery can be achieved by heating to 400°C for 15 minutes or to 440°C for 5 minutes.

REFERENCES

1. Bemski, G. and W. M. Augustyniak, Phys. Rev., 108, 145 (1957).

2. Tomek, K., Czech. J. Phys. B 15, 135 (1965).

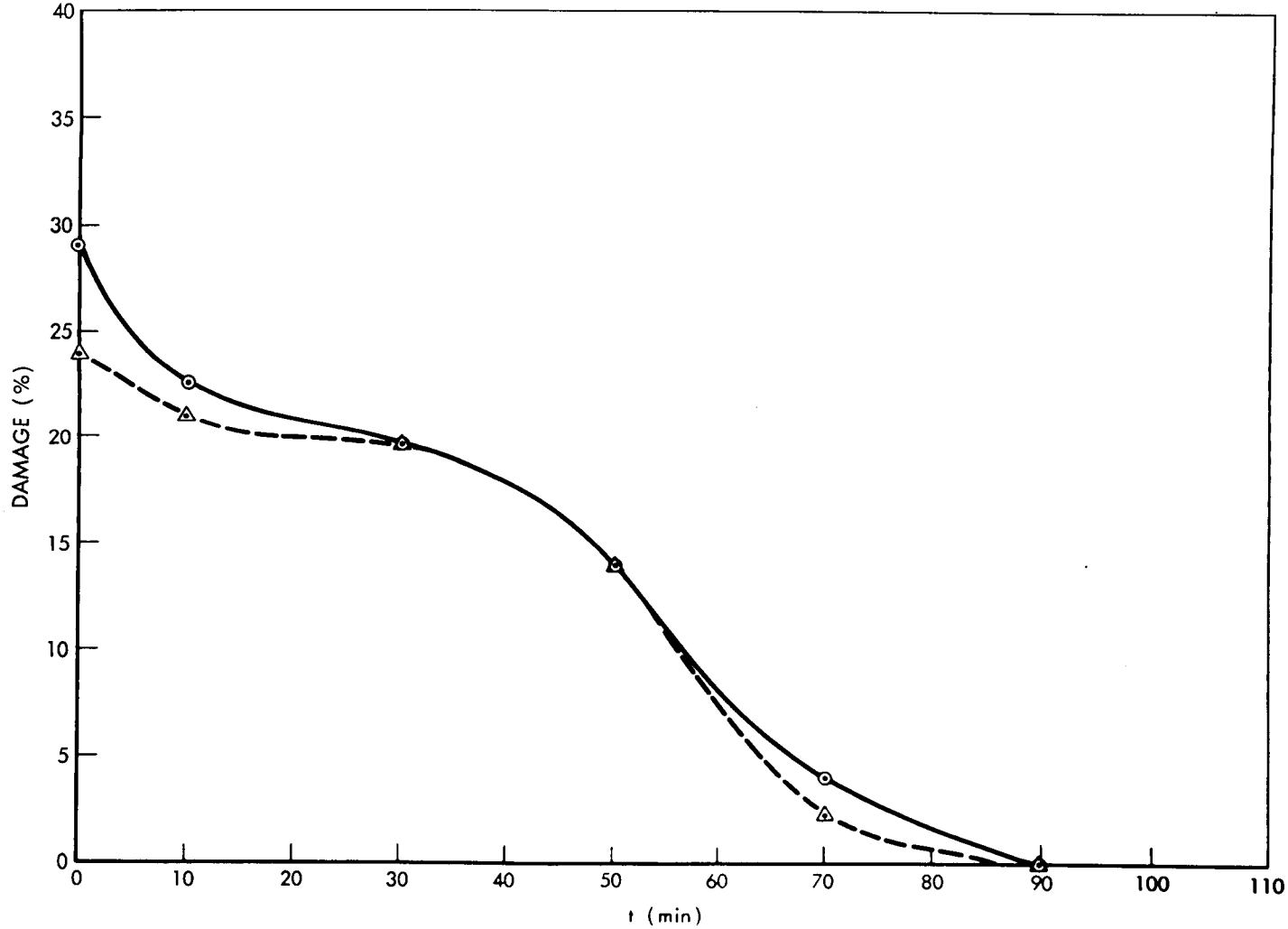

Figure IV-1. Isothermal Annealing at 390°C After 2 Mev, 1.4×10^{14} Electrons/cm^2 Radiation. △ for D_1 and ⊙ for $D\eta$

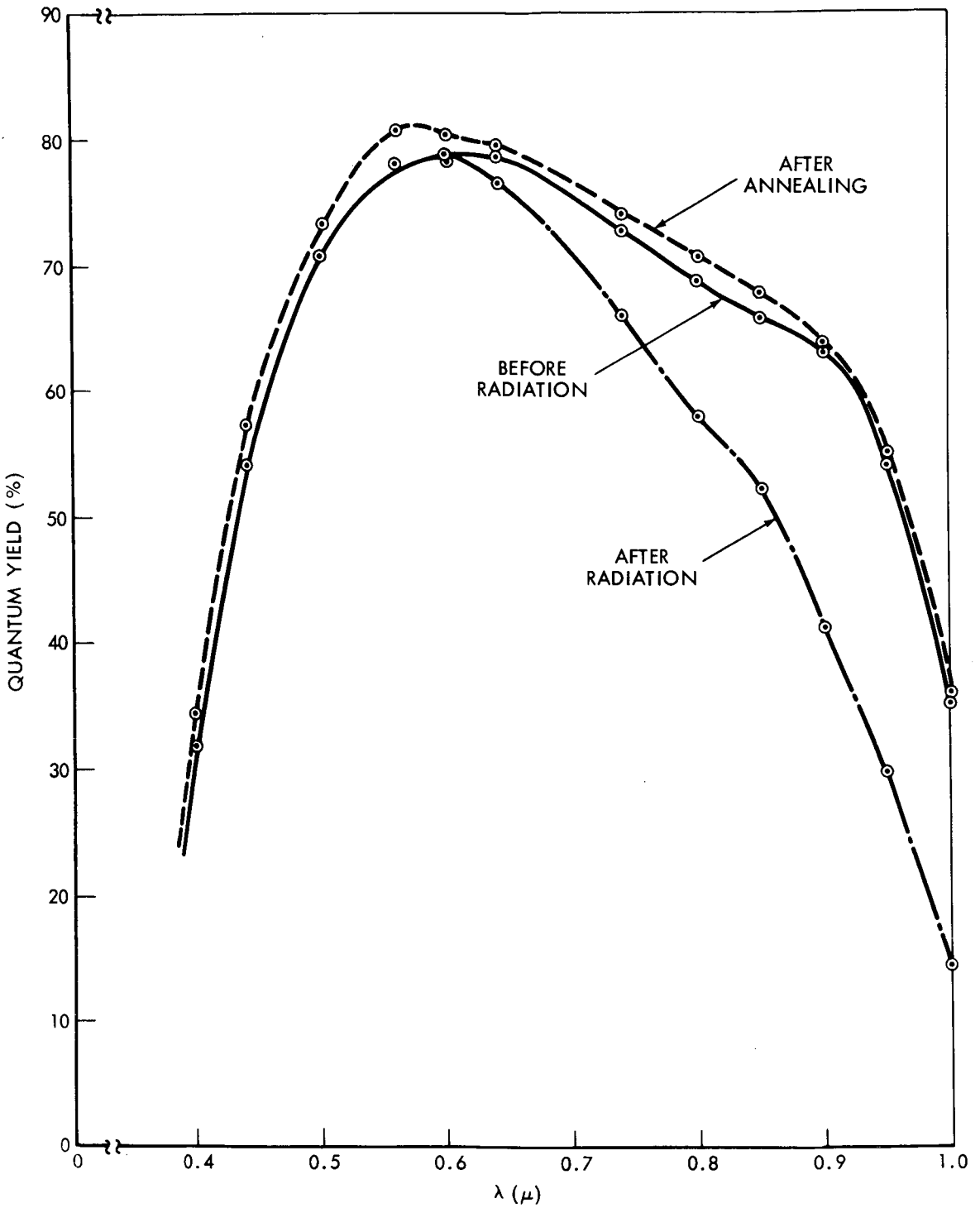

Figure IV-2. Comparison of Quantum Yield of the Solar Cell Before and After the Radiation, and After Annealing, From the Solar Cell of Figure IV-1

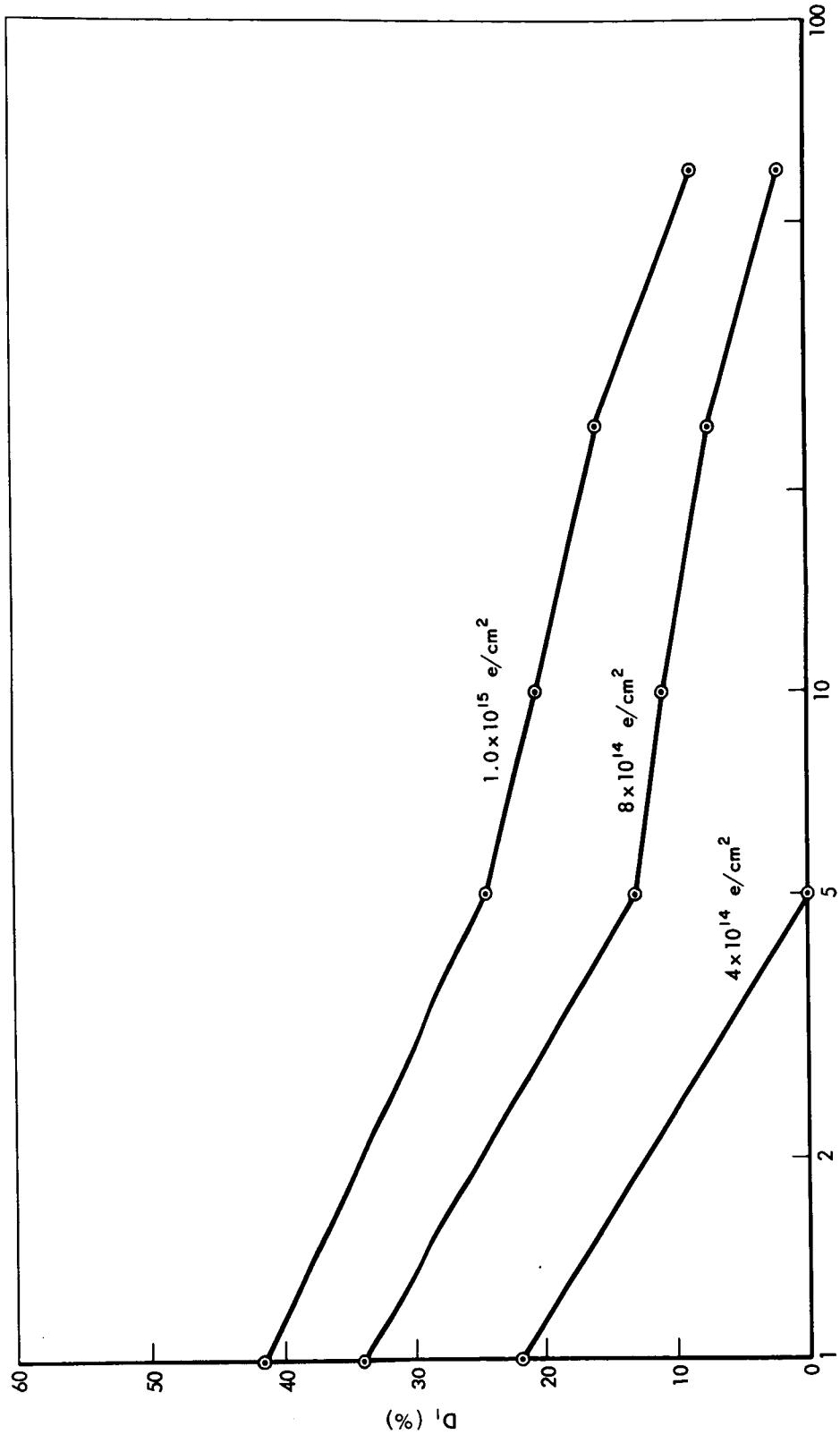

Figure IV-3. Dependence of Isothermal Annealing Characteristics on the Damage Levels

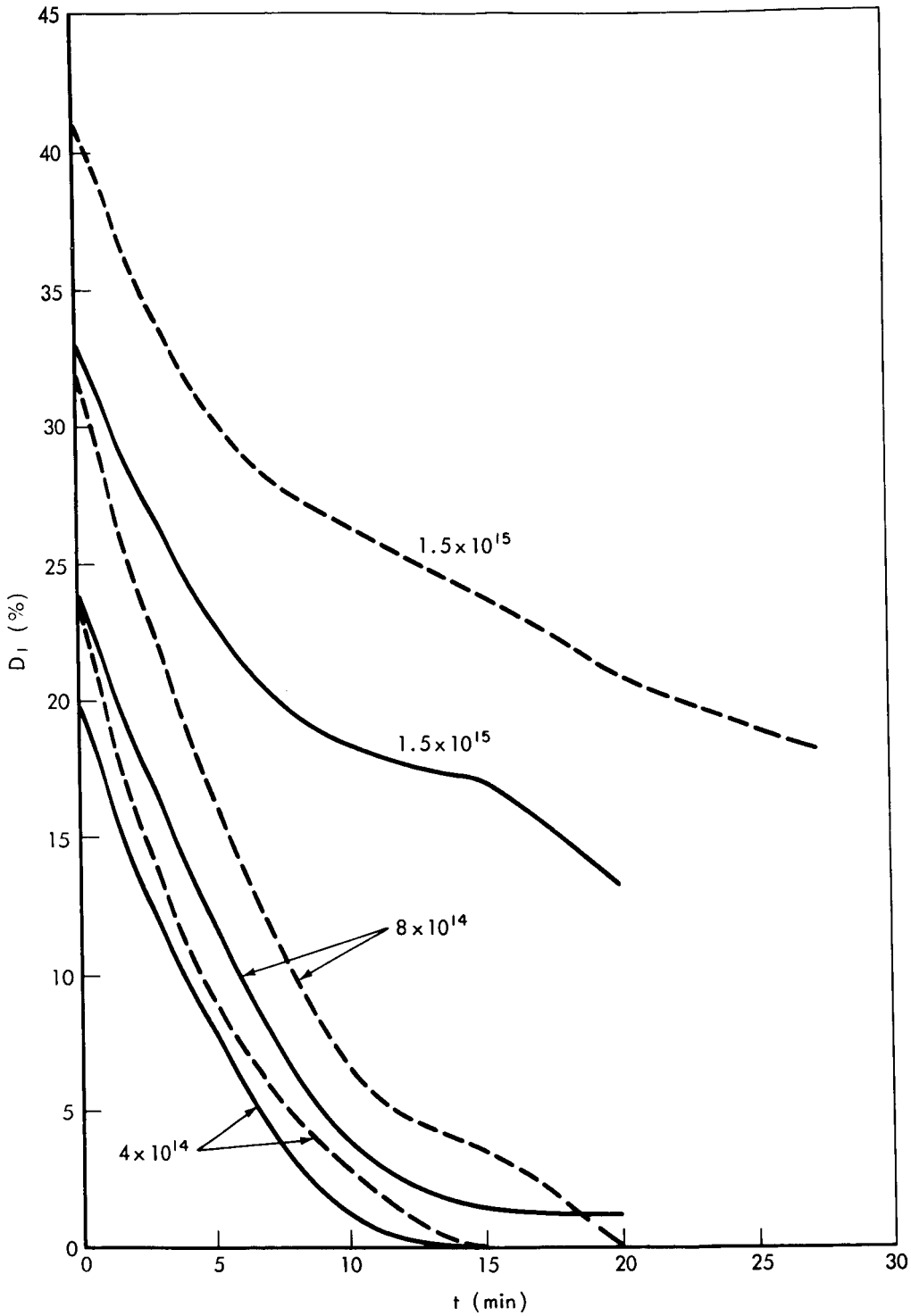

Figure IV-4. Measurement of Damage and Isothermal Annealing with Xenon Light (Solid Curve) and Tungsten Light (Dotted Curve)

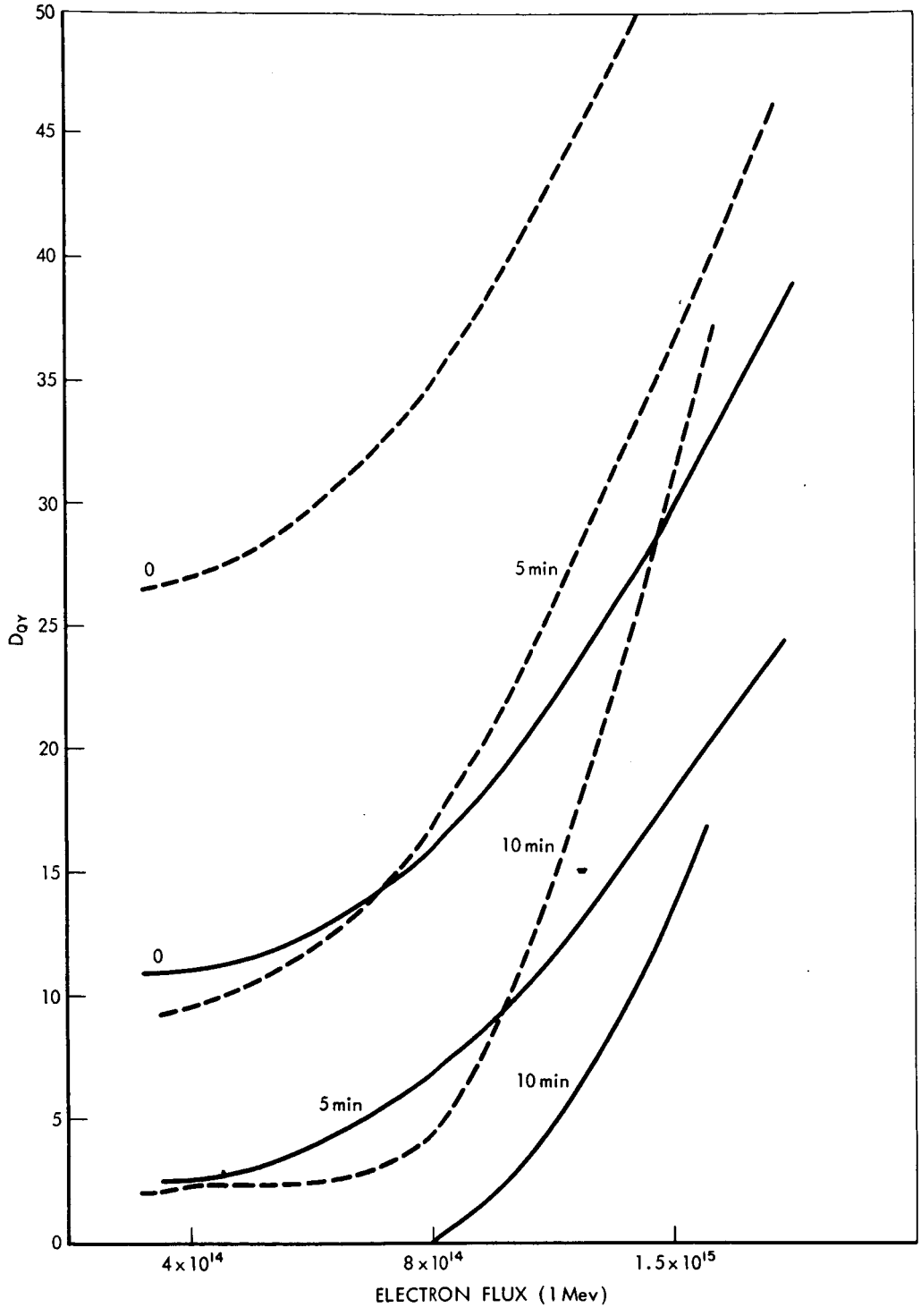

Figure IV-5. Dependence of Isothermal Annealing on the Radiation Damage Measured with 9040 Å (Dotted Curve) and 8020 Å (Solid Curve) Light Source

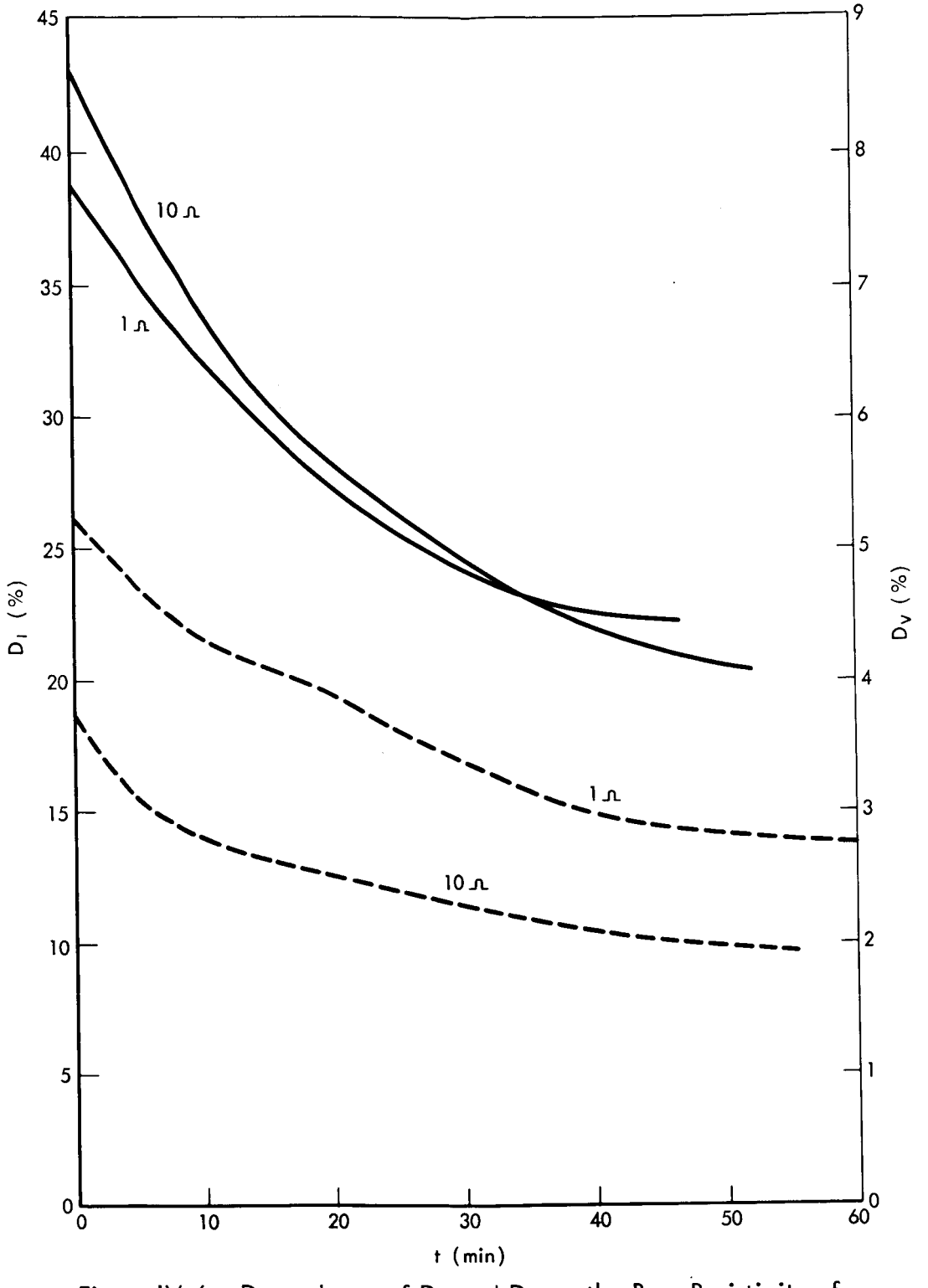

Figure IV-6. Dependence of D_I and D_V on the Base Resistivity of Solar Cells, Annealed at 375° C

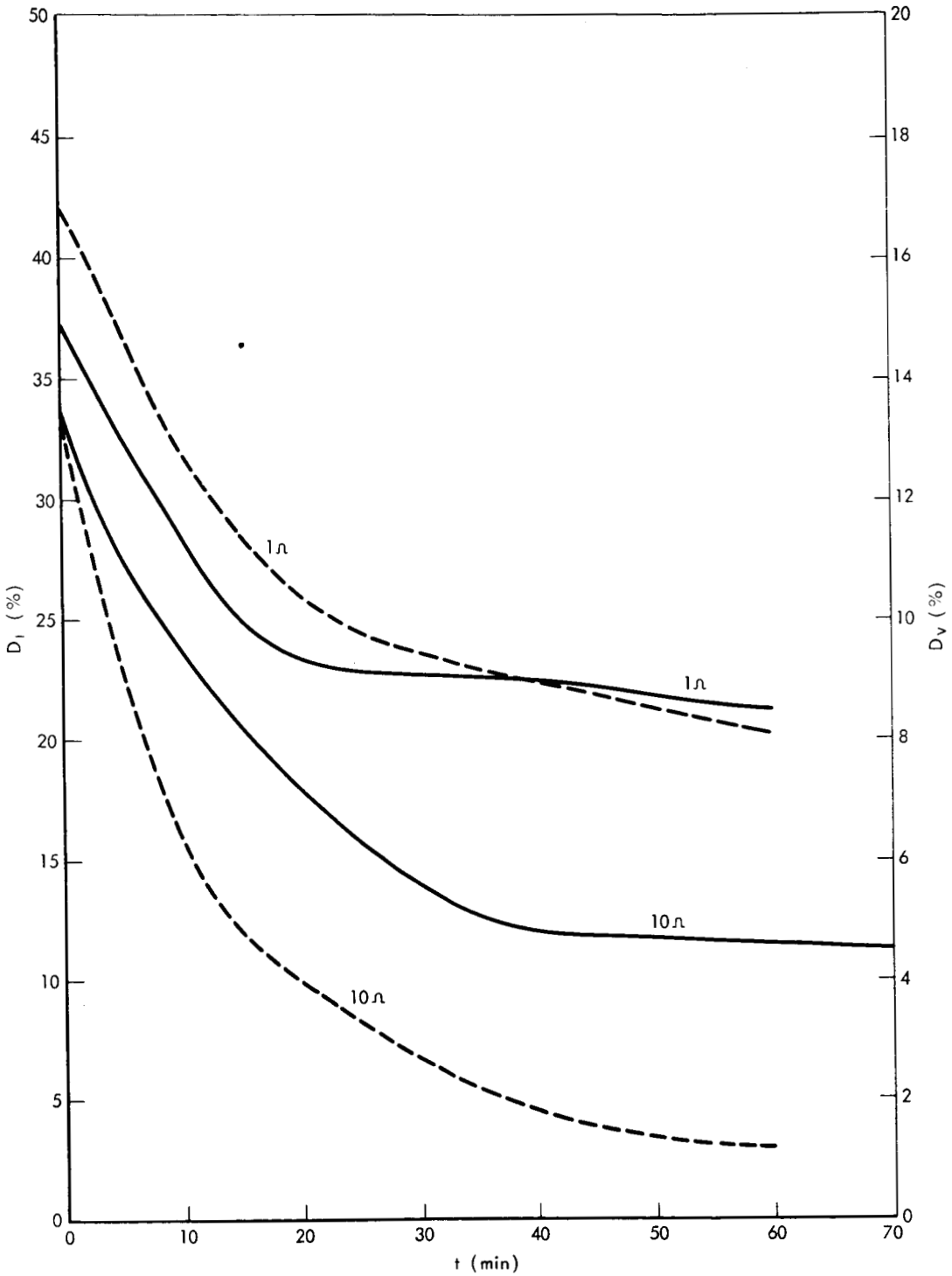

Figure IV-7. Dependence of D_I and D_V on the Base Resistivity of Solar Cells Annealed at 400°C

V. ISOCHRONAL ANNEALING

To investigate the resistivity dependence of annealing behavior, we used solar cells with four different base resistivities: 1, 10, 15, and 25 Ω-cm, respectively. All cells were radiated at 10 Mev, with 1×10^{15} e/cm^2. Isochronal annealing was made for 10 minutes at each temperature. These data are shown in Figure V-1. The annealing curves show the structure of a small annealing stage near 100°C. A reverse annealing is shown at 200°C. This stage is independent of the solar cell resistivity. The last stage of annealing which occurred above 350°C, depends strongly on the solar cell resistivity. Only in 10 Ω-cm cells do we observe a complete recovery at 450°C.

Figure V-2 shows the annealing characteristics for different degrees of initial damage, annealed for 20 minutes at each temperature. We observe the progress of annealing above 340°C and complete annealing at 420°C when the flux level, ϕ, is less than 1×10^{15} e/cm^2. When ϕ is much larger, the isochronal curve shows a tail and a portion of unannealable damage is observed. This tail effect persists at high temperature of from 480°C to 550°C. Higher temperature treatment resulted in additional damage.

The significance of this tail effect will be discussed in Chapter VI. If we plot the value of the unannealable or residual damage, R, as a function of the

flux, we obtain the result shown in Figure V-3. The curves are plotted with the isochronal annealing temperature as a parameter. A threshold of flux level, is obtained at each annealing temperature, above which annealing would not be complete. The true ϕ_t is where the value R=O becomes temperature independent. Allowing for the uncertainty of extrapolation, we arrive at a value of ϕ_t = $1.0 \pm .2 \times 10^{15}$ e/cm^2. We can expect that this value will change for solar cells with different impurity concentration and processing history, and the energy of the radiation source.

For practical application, temperature dependent ϕ_t is interesting because it provides the critical value before which the annealing should be carried out in order to achieve a complete recovery. This is given in Figure V-4. The dotted line is an extrapolation to imply a minimum temperature below which normal annealing cannot be carried out effectively.

In Figure V-5 the spectral response at 0.90μ is given for the data of Figure V-2. Not only the absolute damage—this one observes in all quantum yield data, – but the relative damage also, is higher in Figure V-5 than that of Figure V-2 which is for white light. Furthermore, for the curve of the lowest flux, the apparent annealing temperature for the 0.90μ case is 20°C higher than that of white light. These observations are explained by the following mechanism.

(1) Q (blue region after annealing) > Q (blue region, original)

(2) Q (red region after annealing) ≤ Q (red region, original)

The equality in (2) holds when the solar cell is completely annealed. The inequality (1) is an interesting one that we have observed in many quantum yield data. In future work we will investigate in detail the conditions that establish this inequality. Some indirect evidence shows a reduction in surface recombination when silicon crystals are treated at 450° C for extended periods of time (Reference 1). The improvement over the original solar cell will be amplified when sunlight is used. In this case, there is a greater number of photons in the blue region, therefore, the improvement will be even more pronounced. This is demonstrated in Figure V-6, where two spectral response curves are given, one is the original response, the second is the response after the radiation followed by annealing, based on the data of Figure IV-2. They are now given in equivalent response to the solar light, based on the Johnson spectra data (Reference 2).

To investigate whether a complete recovery can always be achieved when the solar cell is heated up to sufficiently high temperatures, we carried out isochronal annealing up to 650° C (Figure V-7). The isochronal annealing time is 10 minutes at each temperature. We observe complete annealing of 5×10^{13} e/cm^2 radiation and the "tail effect" for 1×10^{16} e/cm^2 radiation. The tail effect persists up to 525° C, then a small annealing stage occurs at 550° C. Above 550° C a reverse annealing occurs for both cells radiated with 5×10^{13} and 1×10^{16} e/cm^2. This is the onset of thermal damage

(Reference 3), and this sets the upper temperature limit where isochronal annealing can be beneficial.

REFERENCES

1. Tomek, K., Czech. J. Phys. B 15, 135 (1965).

2. Thekaekara, M.P., Solar Energy, 9, 7 (1965).

3. Bemski, G. and C.A. Dias, J. Appl. Phys. 35, 2983 (1964); B. Ross, and J.R. Madigan, Phys. Rev. 108, 1428 (1957); C.S. Fuller and R.A. Logan, J. Appl. Phys. 28, 1427 (1958); G.N. Galkin, E.L. Nolle, and V.S. Vavilov, Soviet Phys. Solid State (Transl.) 3, 1708 (1961).

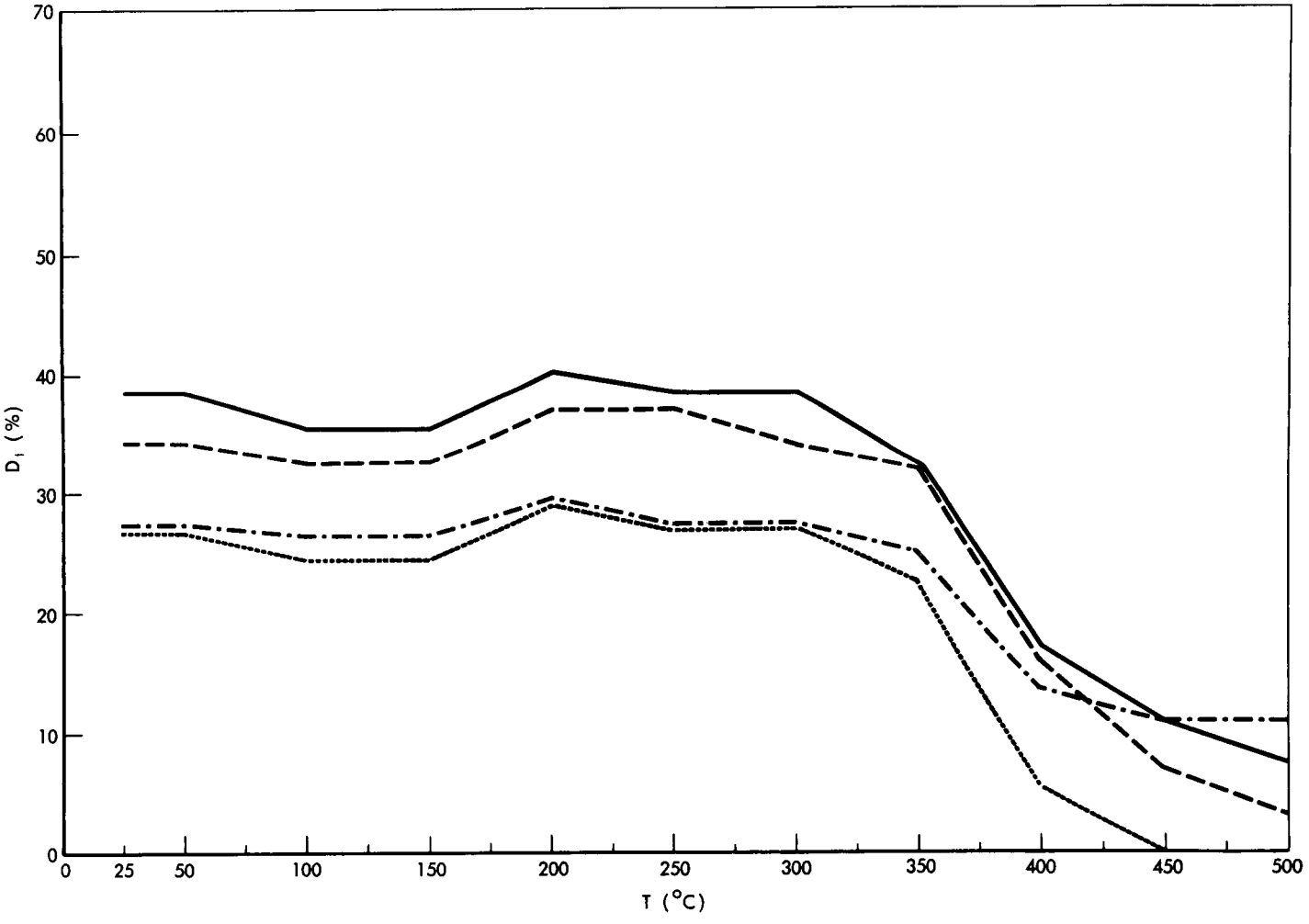

Figure V-1. Isochronal Annealing Characteristics of Solar Cells with Different Base Resistivities; 1Ωcm (———), 10Ωcm (------), 15Ωcm (— — —) and 25Ωcm (—·—)

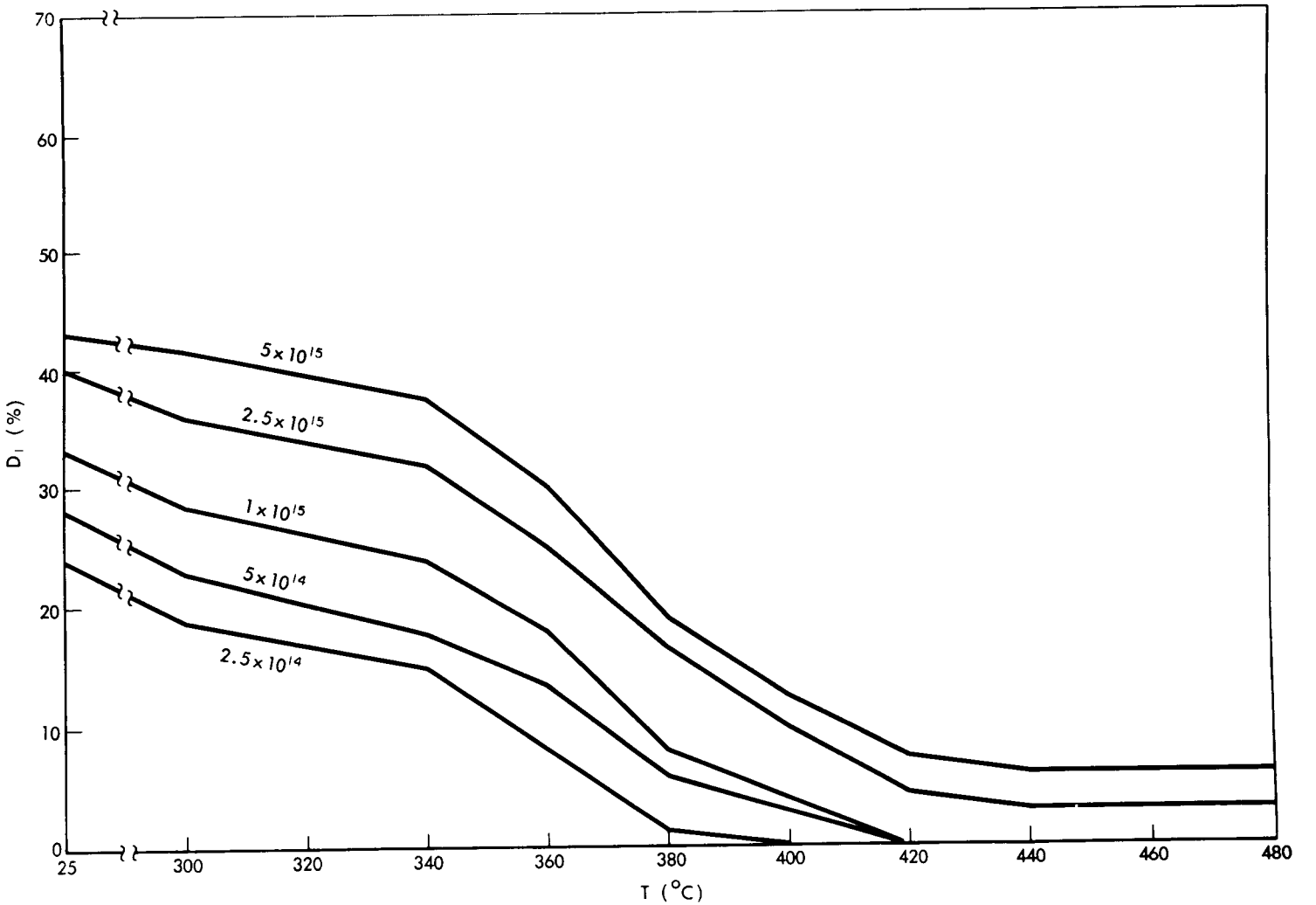

Figure V-2. Isochronal Annealing Characteristics of Solar Cells of 10Ωcm Base Resistivity of Different Initial Damage States

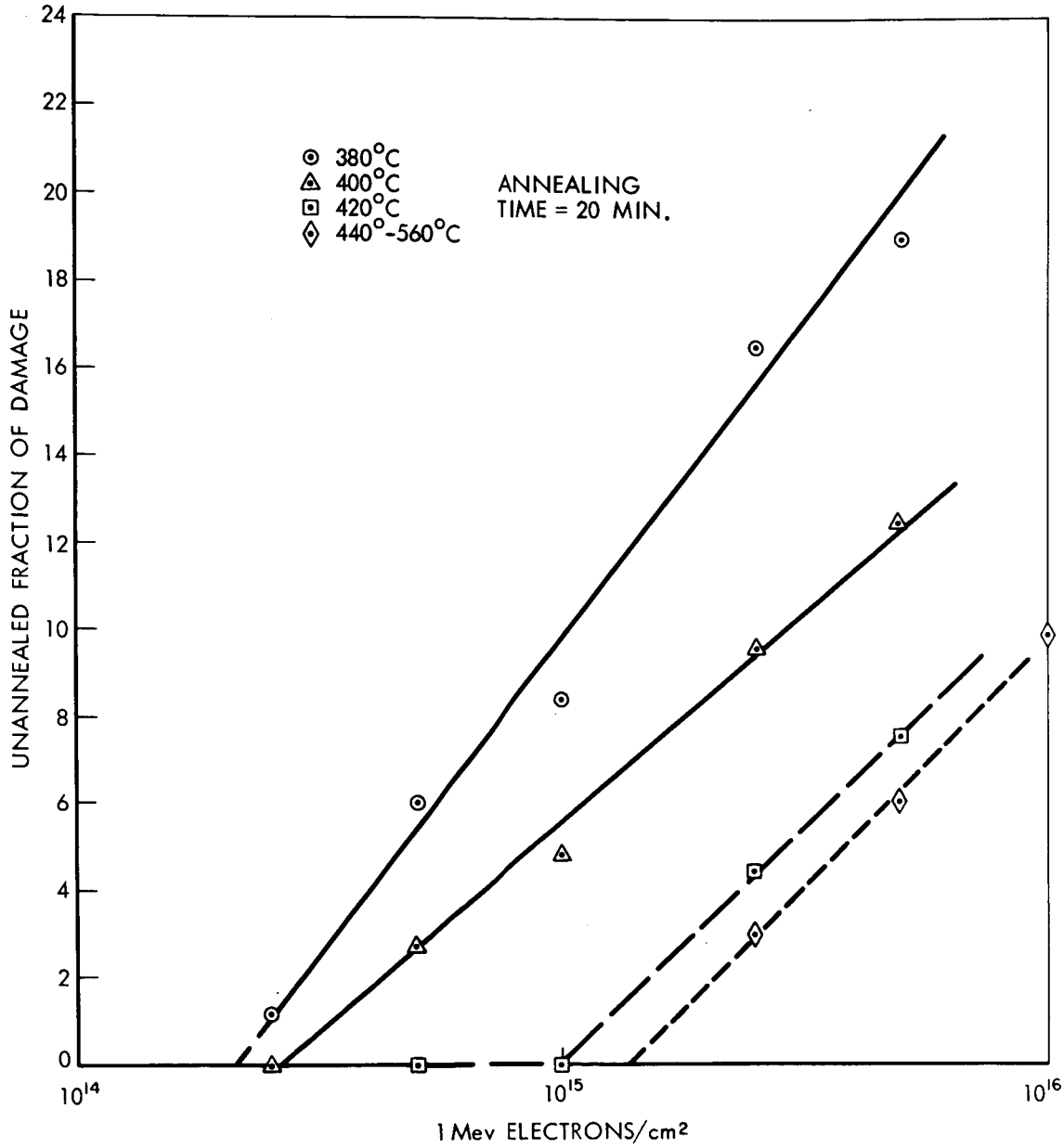

Figure V-3. Dependence of Unanneable Damage on the Initial Damage, with the Isochronal Annealing Temperature as the Parameter

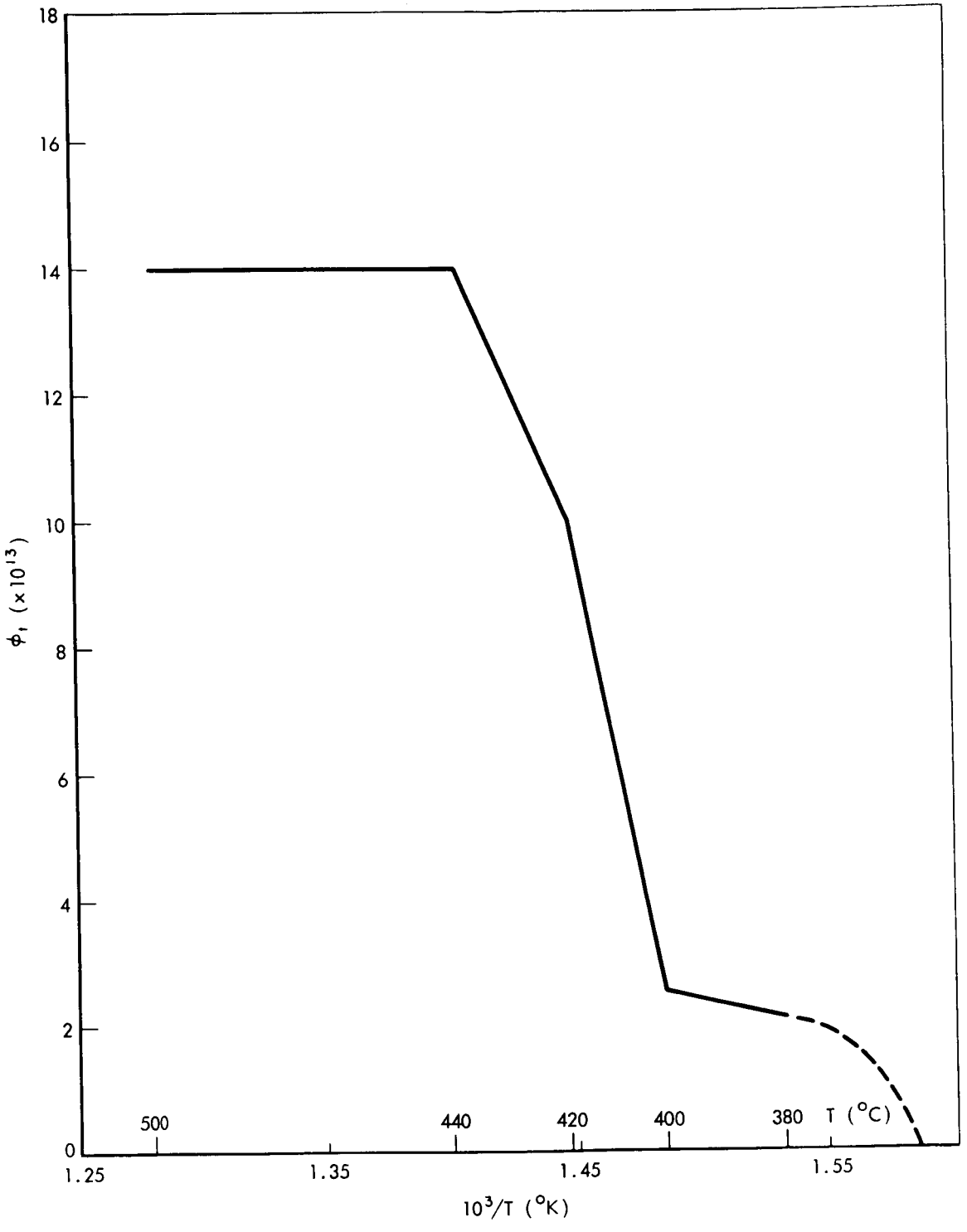

Figure V-4. Temperature Dependence of the Threshold of Unanneable Damage

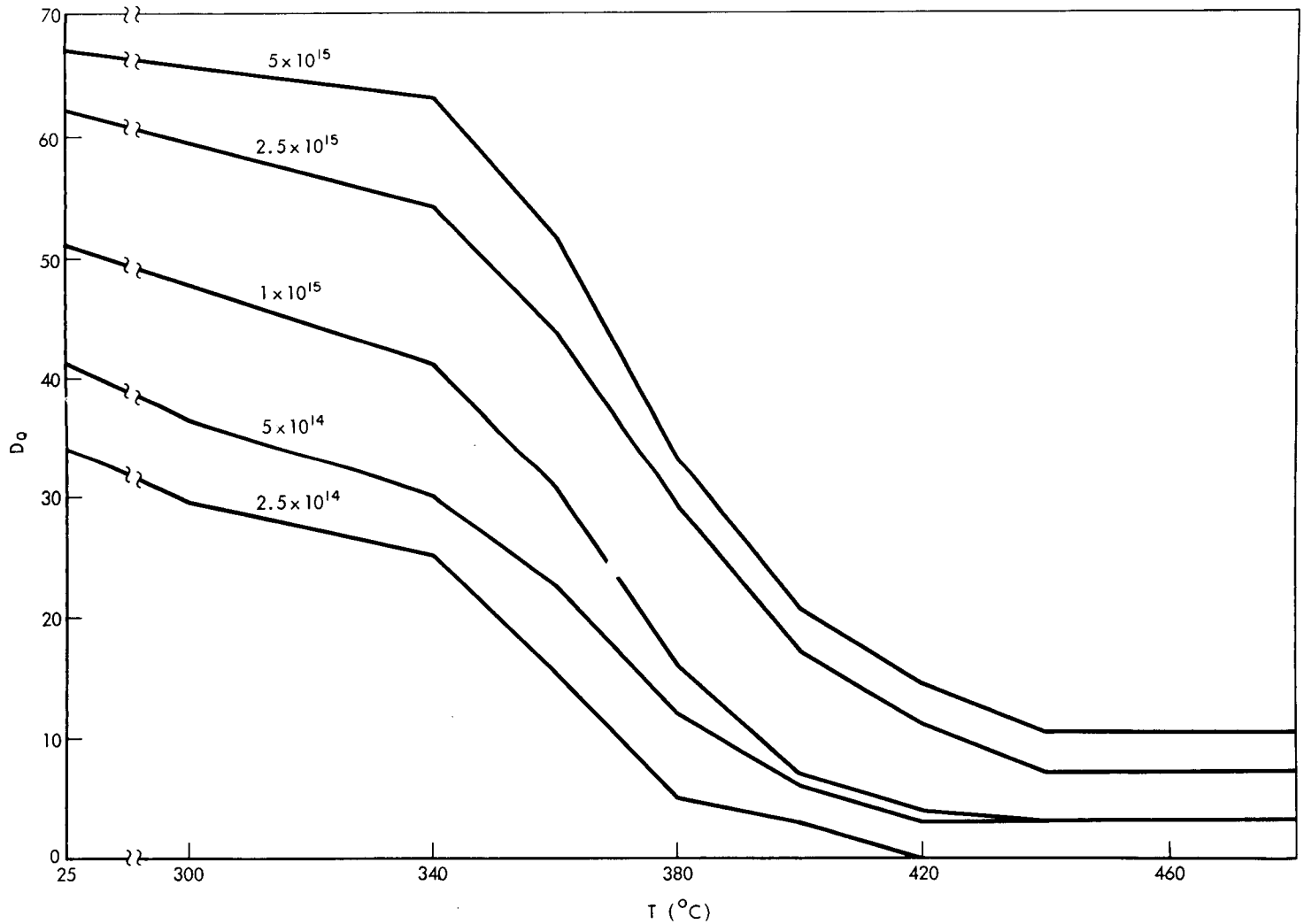

Figure V-5. Isochronal Annealing of Solar Cells of 10Ωcm Base Resistivity with Different Initial Damage, Measured with 9000 Å Light Source

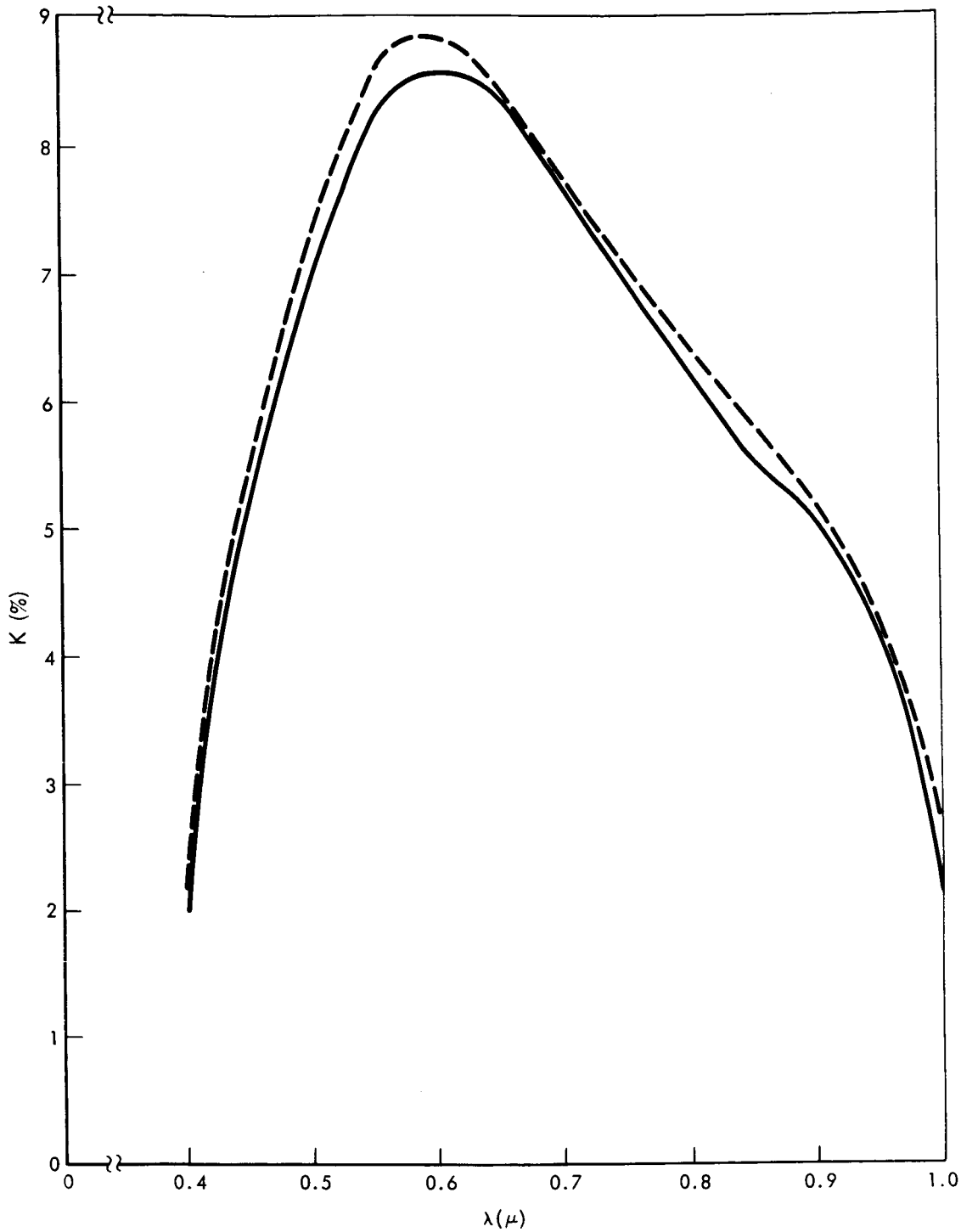

Figure V-6. Response of an Annealed Solar Cell to the Johnson Spectra of Solar Light Sources. Original Response (———); Response After Radiation and Followed by Annealing (– – –). (Data of Solar Cell from Figure IV-2)

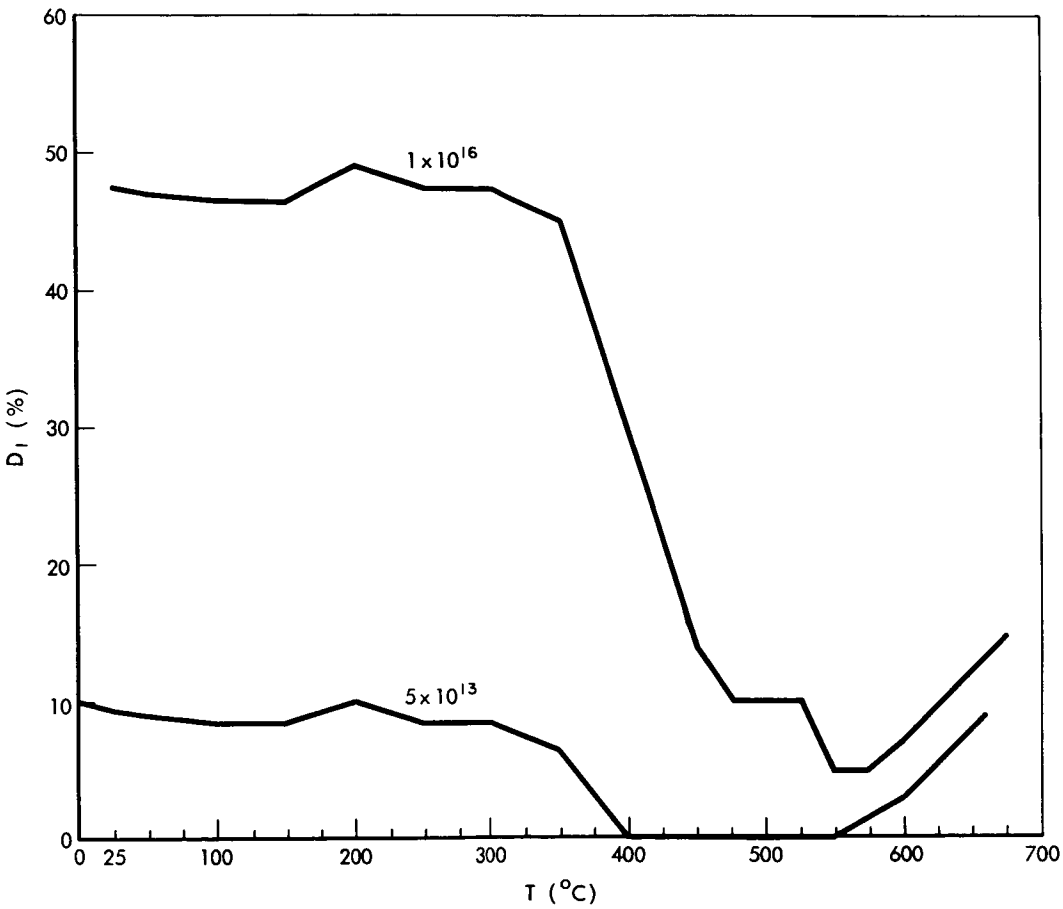

Figure V-7. High Temperature Isochronal Annealing

VI. REPEATED RADIATION AND ANNEALING

In connection with the observation of unannealable residual damage when the flux level of radiation is larger than a critical value, we found that if we interrupt the radiation and carry out intermediate annealing, annealing can still be complete at a total accumulated flux level higher than the threshold value discussed in the previous chapter. Thus far, we have repeated the process seven times with 4×10^{14} e/cm^2 radiation, a total flux 2.8 times the threshold value, and have not found, within an experimental margin of error ±3%, any unannealable damage as shown in Figure VI-1. In the same figure, radiation damage characteristics are given for solar cells with a drift field structure, with Li doping, with B and Al as p-type impurities.

The cyclic radiation and annealing experiment will be continued because it will establish an upper limit for the rejuvenation of solar cells by annealing. In what follows, we will discuss some physical implications of this limit and a proposed explanation.

In the ordinary thermodynamics of annealing as extensively used in the study of defects in metals (Reference 1), two assumptions are inherent: (1) the reversibility of annealing and radiation damage, and (2) the validity of the superposition principle; i.e., the number of defects is proportional to the radiation flux.

In Figure V-2, we have shown that radiation damage and annealing are irreversible when the flux level exceeds a threshold value. Furthermore, the completeness of annealing depends on the extent of damage. When we assume that the superposition principle is invalid. Therefore, the ordinary concept of characteristic values of isothermal annealing time, isochronal annealing temperature and the resultant kinetic energy cannot be applied. We propose intuitively the following process which will result in the above interaction.

The stability of the defect is controlled by two factors:

1. The interaction between the regular lattice and the defect.
2. The interaction between the defects.

The first type of interaction involves single defects (SD) and applies to extremely dilute defect concentrations, such as Schottky defects, where the number of defects introduced by radiation damage does not exceed the defect density allowed by the thermodynamical state of the regular lattice. This type of effect is simple and can be governed by first or lower order kinetics.

For the second type of interaction, the process is much more complicated and denser defects are involved. There is a van der Waal attraction between the defects, and a repulsion between the lattice and the defect. When a cluster is less than about 10 lattices in dimension, the defect is termed a small cluster defect (SCD). The repulsive force due to thermal stress may be even larger

than in the case of dilute, uniformly distributed defects. The result is a dissociation of the cluster at temperatures even lower than the annealing temperature. We attribute the reverse annealing observed near 200° C to this process.

The distance between small clusters as proposed in our model is less than the mean free path of the minority carrier, or about 10^{-5} cm. Therefore, SCD as a trapping or recombination center is manifested as a much smaller number of defects but is multiplied in the reverse annealing process.

The extreme case of high defect density occurring in a large dimension of the crystal will be termed large cluster defects (LCD). In such a case, the defects themselves constitute a thermodynamically regular lattice structure and have a high resistance against thermal annealing.

During radiation with a flux ϕ, we have the following scheme of interactions and reactions:

1. $\phi \rightarrow$ SD, SCD, and LCD,
2. SD $\rightleftharpoons$ SCD,
3. SD $\rightarrow$ LCD,
4. SD $\rightarrow$ annealing,
5. SCD $\rightarrow$ SD $\rightarrow$ annealing,
6. LCD $\not\rightarrow$ annealing.

In 1 the production of SCD is equal to zero. This conclusion is drawn because there was reverse annealing at room temperature but not at liquid nitrogen temperature. Therefore, an SCD occurs from the thermal interaction and it is not a primary defect. In 2 the forward process is not definitely established, but we attribute the reverse process to the manifestation of the reverse interaction. Process 3 was not directly observed, but the differences in the unannealable radiation damage between specimens radiated at different temperatures is consistent with this process.

In annealing, at least for a flux level of radiation which is not excessive, process 4 is most important. Process 5 represents only about 10 percent of the interactions. The intermediate step of process 5 is reverse annealing. Finally, phenomenologically, we have to assume that the forward process of 6 is zero, that is, that the LCD cannot be annealed.

From the above scheme, we see the importance of the role of the SCD in explaining many experimental observations. The energy of dissociation of this process will be determined in the course of time.

The complicated annealing schemes require a flux-dependent reaction rate in the anneal equation. This has not been developed at present, especially for SCD and LCD. We note that the LCD mechanism can also be used to explain the difficulty in the annealing of proton damage, which will be discussed in Chapter X.

In conclusion, we should emphasize a main difference in the effective state of the semiconductor under discussion from that of a metal. While the defects of metals can be characterized by interstitials and vacancies, semiconductor defects at room temperature are always complex defects, that is, interstitials and vacancies associated with impurities with a definite structure. On the other hand, the mechanism proposed here is not a new type of structure, but rather a pure geometrical consideration of these defects. Further investigation of this mechanism will be carried out by a comparative study of the damage due to radiation of different types and energies, as well as the dependence of damage on the temperature of solar cells during radiation.

REFERENCE

1. Damask, A.C. and G.J. Dienes, Point Defects in Metals (Gordon and Breach Pub., 1964).

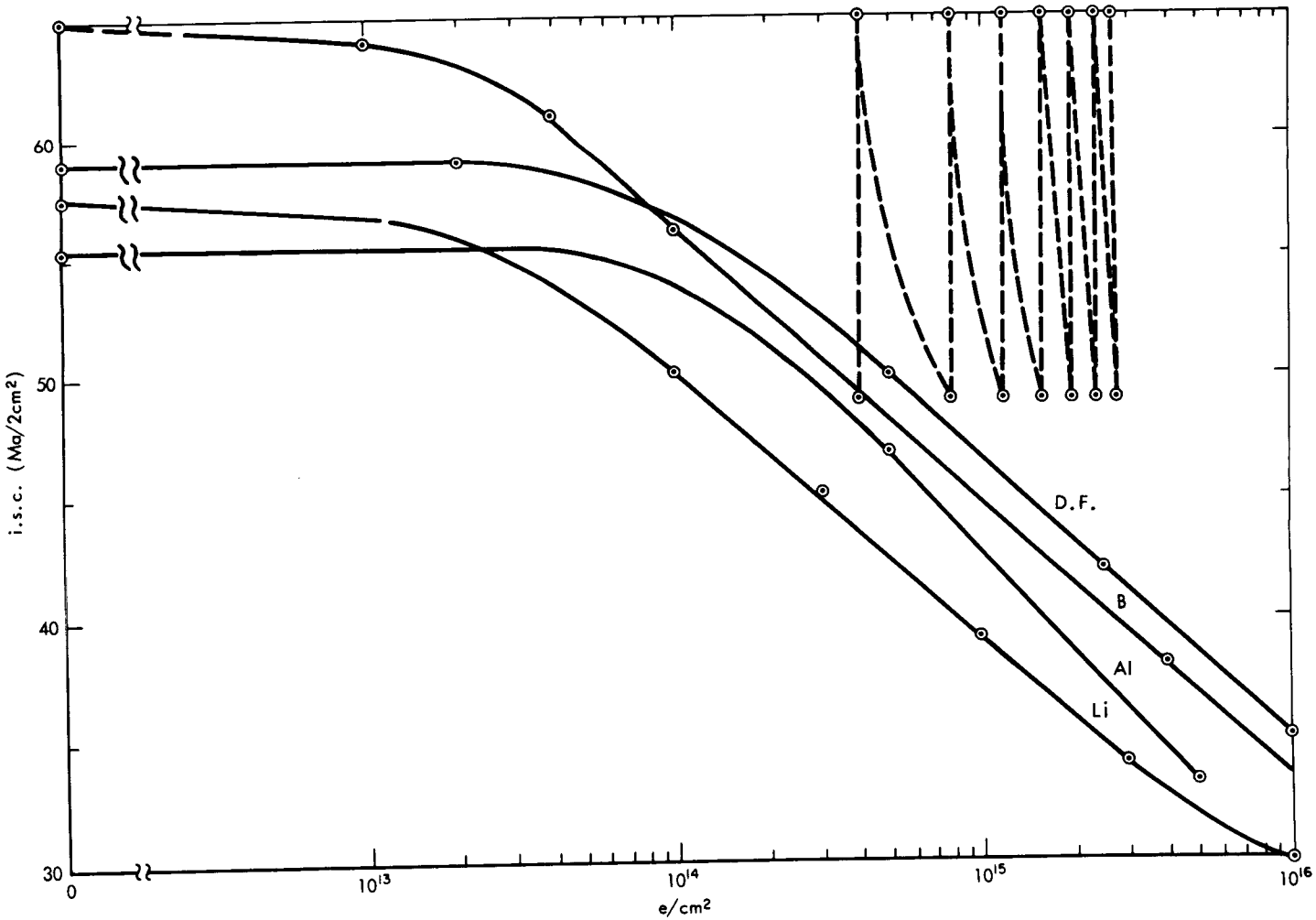

Figure VI-1. Degradation of Short Circuit Current of Solar Cells. Solid Curves are for Different Types of Solar Cells. Dotted Curve is for an Ordinary 10Ωcm N and P Solar Cell with Repeated Annealing each time After 4×10^{14}, 1 Mev el/cm² Radiation

VII. ANNEALING OF SEVERAL TYPES OF SOLAR CELLS

In this chapter some preliminary experiments on the annealing of three types of solar cells are presented: lithium-diffused, drift field, and aluminum-doped solar cells.

A. Lithium-diffused Solar Cells

The physical principal of the solar cell with lithium diffusion has been described briefly in Chapter I. Data from surface barrier diodes with lithium diffusion show an improvement in the radiation resistivity of the minority carrier diffusion length (Reference 1). Solar cells with lithium introduced into the P-region through the under side of the solar cell have been fabricated in the RCA Mountain Top Laboratory in cooperation with the basic research group at the RCA Princeton Laboratory (Reference 2). Since this represents preliminary work, definite conclusions should not be drawn. This result is shown in Figure VII-1. Compariwon with typical results such as those of Figure V-2 indicates that the radiation resistance of lithium solar cells is not much improved, at least up to a flux of 5×10^{14} e/cm^2. One disappointing feature is the difficulty of annealing, which is difficult to understand when one considers the high mobility of the lithium ion. If it would interact with the defects introduced by radiation, one would expect annealing at a lower temperature. Comparing the results with the data in Figure V-1, we observe an appreciable increase in the effectiveness of low temperature annealing below about 150° C. But a similar reverse annealing is

observed above 200° C. Complete annealing is obtained only for a flux level of 1×10^{14} e/cm^2 at the high temperature of 500° C. For a flux of 5×10^{14} e/cm^2, the tail effect of unannealable damage is observed. In Figure III-4 the flux is 4×10^{14} e/cm^2 and complete annealing occurs at 400°C. Figure III-5 shows a threshold of the tail effect occurring above a flux of 1×10^{15} e/cm^2. Therefore, at present, the annealing of lithium-diffused solar cells is not encouraging.

B. Drift Field Solar Cells

We have studied drift field solar cells for some time, mostly from the standpoint of their radiation resistance. A report on this aspect of the work is under preparation. For purposes of the present comparative annealing study, we used two solar cells supplied by Texas Instruments, Inc. (Reference 3). The data are given in Figure VII-2. An appreciable improvement in radiation damage resistance of these cells was observed. This will be obvious when results are compared with those of Figure VII-1 for the same level of radiation.

This is also true when compared with the data of Figure VII-3. However, this comparison is based on the relative value of damage. Usually the drift field solar cell has a lower initial efficiency, and on an absolute base, the short circuit current of the drift field solar cell is lower than that of the ordinary solar cells such as those used in Figure V-2*.

*Only very recently, a cross-over has been observed, that is, after a flux level of 2.5×10^{14} e/cm^2 damaged drift field solar cells, prepared by Texas Instruments, Inc. (Reference 3), become better than the cells of the kind used in Figure V-2.

The required annealing temperature for the drift field solar cell is higher than that shown in Figure V-2. Two conceivable causes of the increase of the required annealing temperature are: (1) the excessive impurity concentration introduced in establishing the concentration gradient will result in many defect-forming centers, and (2) the temperature treatment to form the drift field concentration profile in addition to that required for the usual P-N junction formation process could introduce thermal damage in addition to the radiation-produced defects.

Therefore, the drift field solar cell indeed may not be suitable for annealing purposes.

C. Aluminum Doped Solar Cells*

The purpose of studying the annealing of aluminum-doped solar cells is to investigate the effect of impurities on annealing effectiness and annealing temperatures. In this case, we will compare aluminum-doped and boron-doped solar cells. Figure VII-3 indicates that for aluminum-doped cells, as in the case of boron-doped cells (Figure V-1), the 10-Ωcm base resistivity is better than 1Ω-cm base resistivity, both from the standpoint of radiation resistance and annealing effectiveness. Up to now we have only phenomenological data. A theoretical understanding of the cause will be very important in the development of solar cell technology. With respect to annealing, it seems that the

*These cells were obtained through the courtesy of Mr. R. Cole of Texas Instrument, Inc.

aluminum-doped solar cell generally requires a higher annealing temperature than the boron-doped cell.

REFERENCES

1. Vavilov, V.S., S.L. Smirnor, and V.A. Chapnin, Soviet Phys. Solid State (Transl.) 4, 830 (1962).
2. Under Contract NAS5-3788 and NAS5-3686.
3. Under Contract NAS5-9609.

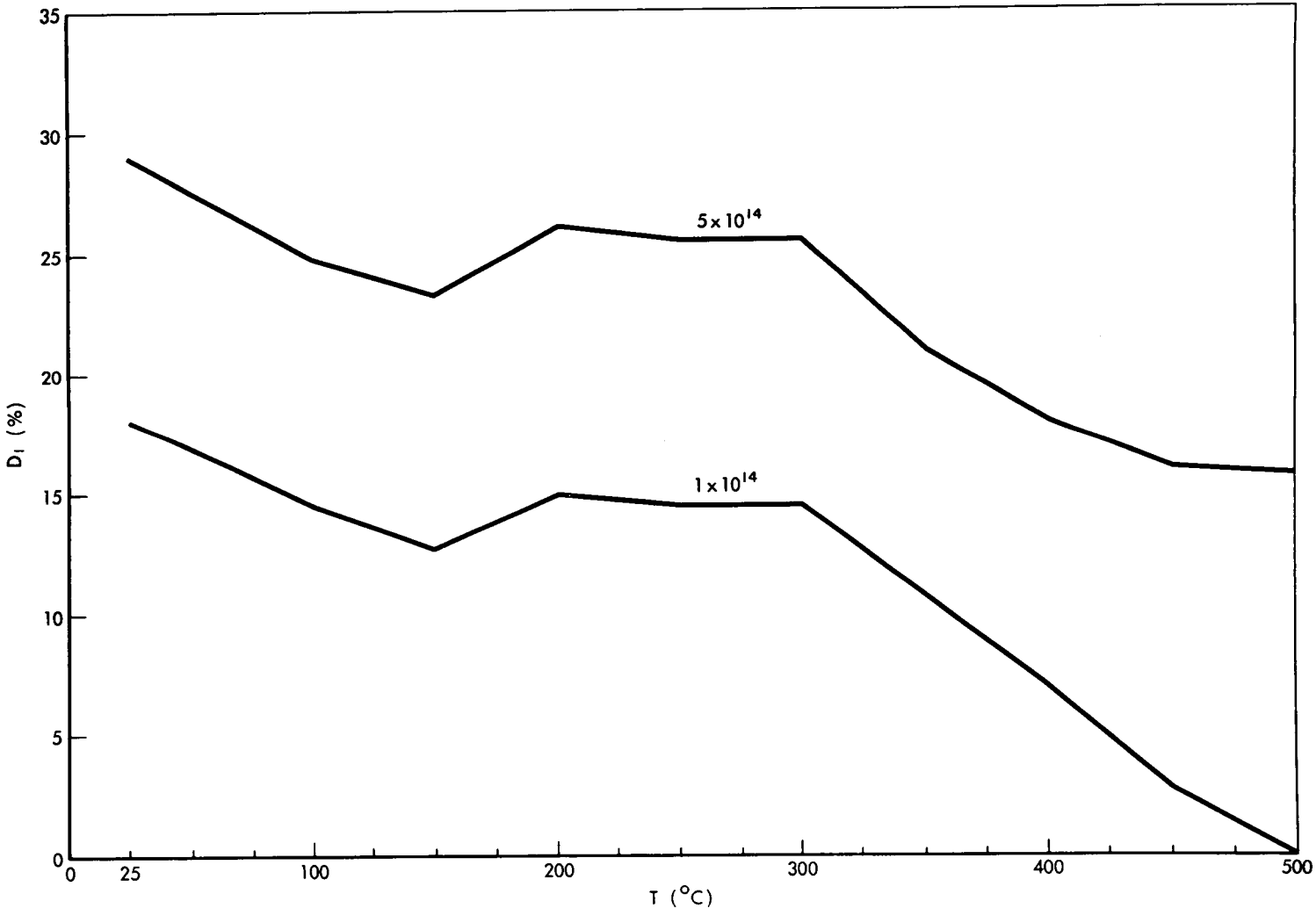

Figure VII-1. Isochronal Annealing of Li Doped Solar Cells with Two Different Initial Damages

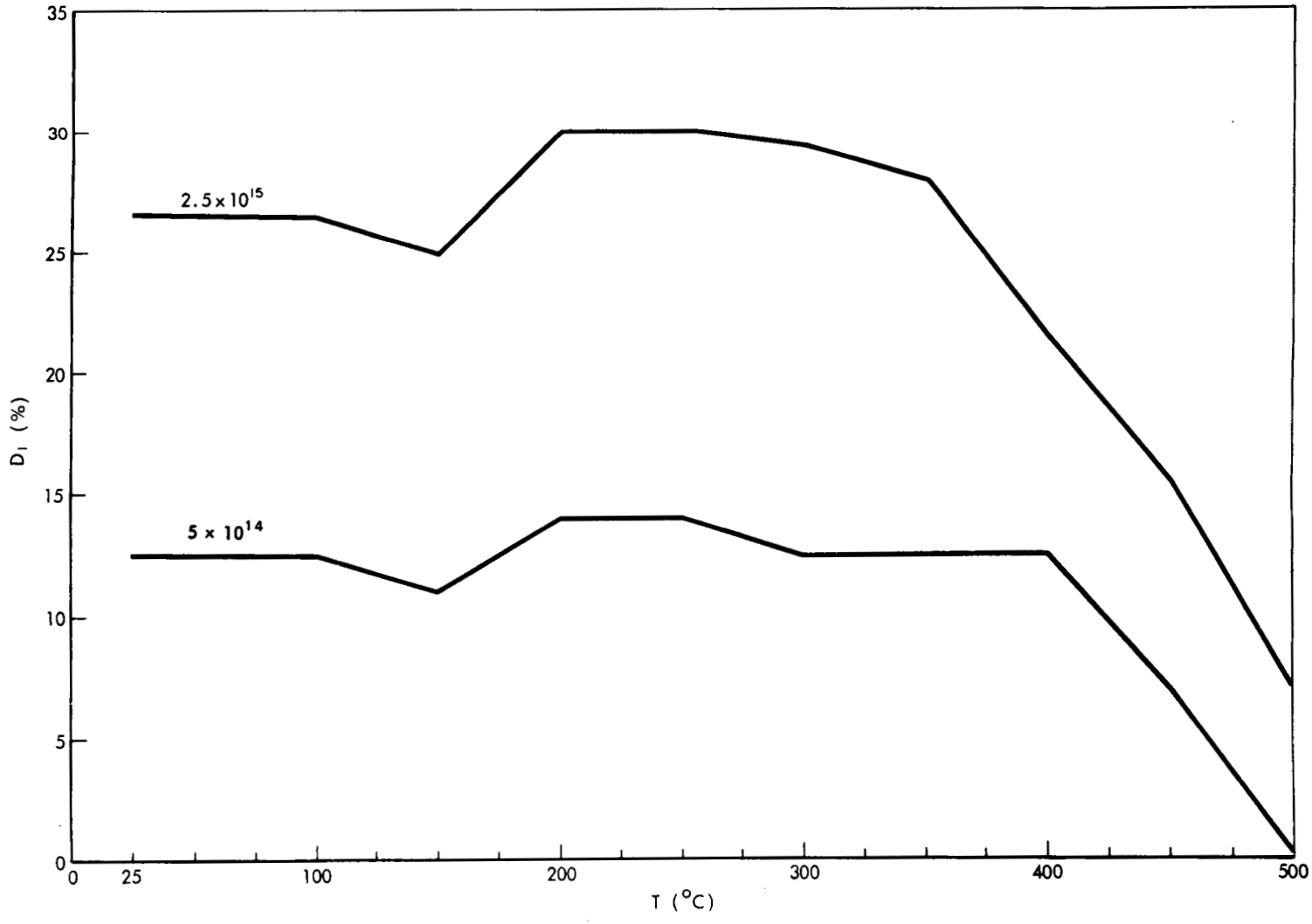

Figure VII-2. Isochronal Annealing of Drift Field Solar Cells with Two Different Initial Damages

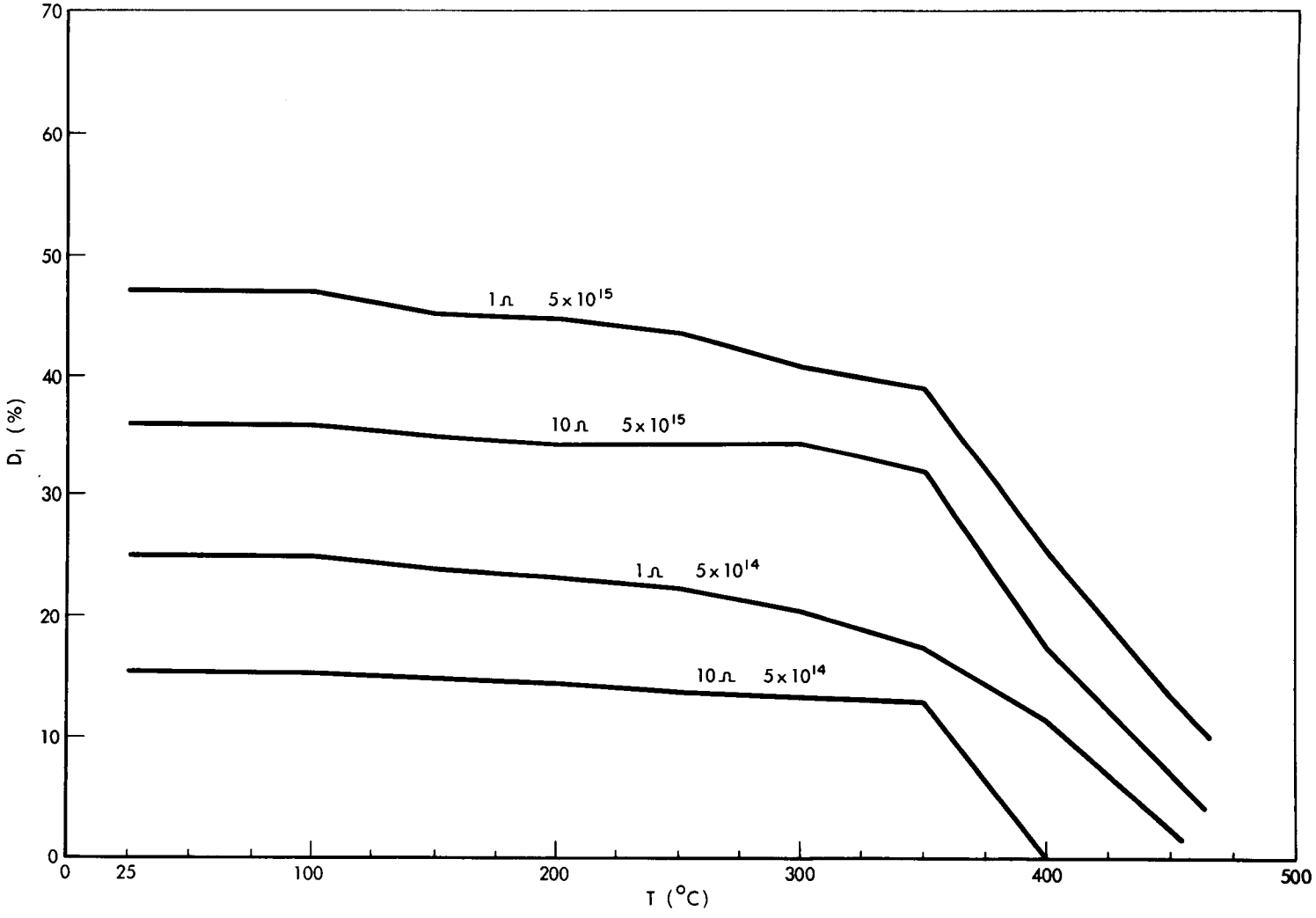

Figure VII-3. Isochronal Annealing of Al-Doped Solar Cells with Different Base Resistivities and Different Initial Stages of Damage

VIII. ANNEALING OF P/N SOLAR CELLS

As is known, in N-type silicon, one mechanism of radiation damage is the production of E-center defects, a neutral charge defect consisting of a vacancy trapped to a substitutional phosphorous atom. Because of its charge state, the E-center may not act as an effective trapping center (Reference 1). However, the effect of the defect as an impurity scattering center on mobility can be important, as our measurement is a composite effect of carrier density and mobility. One interesting prospect is that if the E-center is a dominant center in the degradations of the photovoltaic generation of P/N solar cells, one should be able to recover much of the damage near 200°C, instead of at 400°C as in N/P solar cells.

Three kinds of P/N cells were used in the present study:

1. IRC P/N cells which were fabricated in 1961 or 1962 and have a 1 Ω-cm base resistivity, with soldered contact on the base.
2. RCA Mountain Top Laboratories cells with 37Ω-cm base resistivity and Ag-Ti alloy base contact.
3. Same cells as 2, except that the resistivity is 1Ω-cm.

All crystals are grown by the Czochralski method and therefore have a high oxygen content. E-center production will become dominant only when the concentration of the impurity content is higher than that of the oxygen content

(Reference 1); therefore, these specimens are, in spite of their representation as practical solar cells, not ideal for a study of the E-center defect.

In specimens 1 and 3, no appreciable annealing is observed in the temperature range from room temperature to 400° C (Figure VIII-1). This may be explained by its rich oxygen content.

A stage indicative of E-center annealing is observed in specimen 2 (Figure VIII-2). Since both specimens 2 and 3 are supplied by the same source and prepared with the same thermal treatment, it is rather strange that specimens of higher resistivity, and therefore lower impurity concentration, should show larger E-center density. The possible explanation is that specimen 2 has not been exposed to a sufficiently high electron flux, since the highest flux used was 5×10^{13} e/cm^2, while the lowest flux used for specimen 3 was higher than 1×10^{14} e/cm^2. This part of the experiment is not complete because of a scarcity of P/N specimens from current industrial production. It would be interesting to explore the rate of E-center production by investigating the annealing of better controlled P/N solar cells.

REFERENCE

1. Watkins, G.D. and J.W. Corbett, Disc. Faraday Soc. No. 31, 86 (1961).

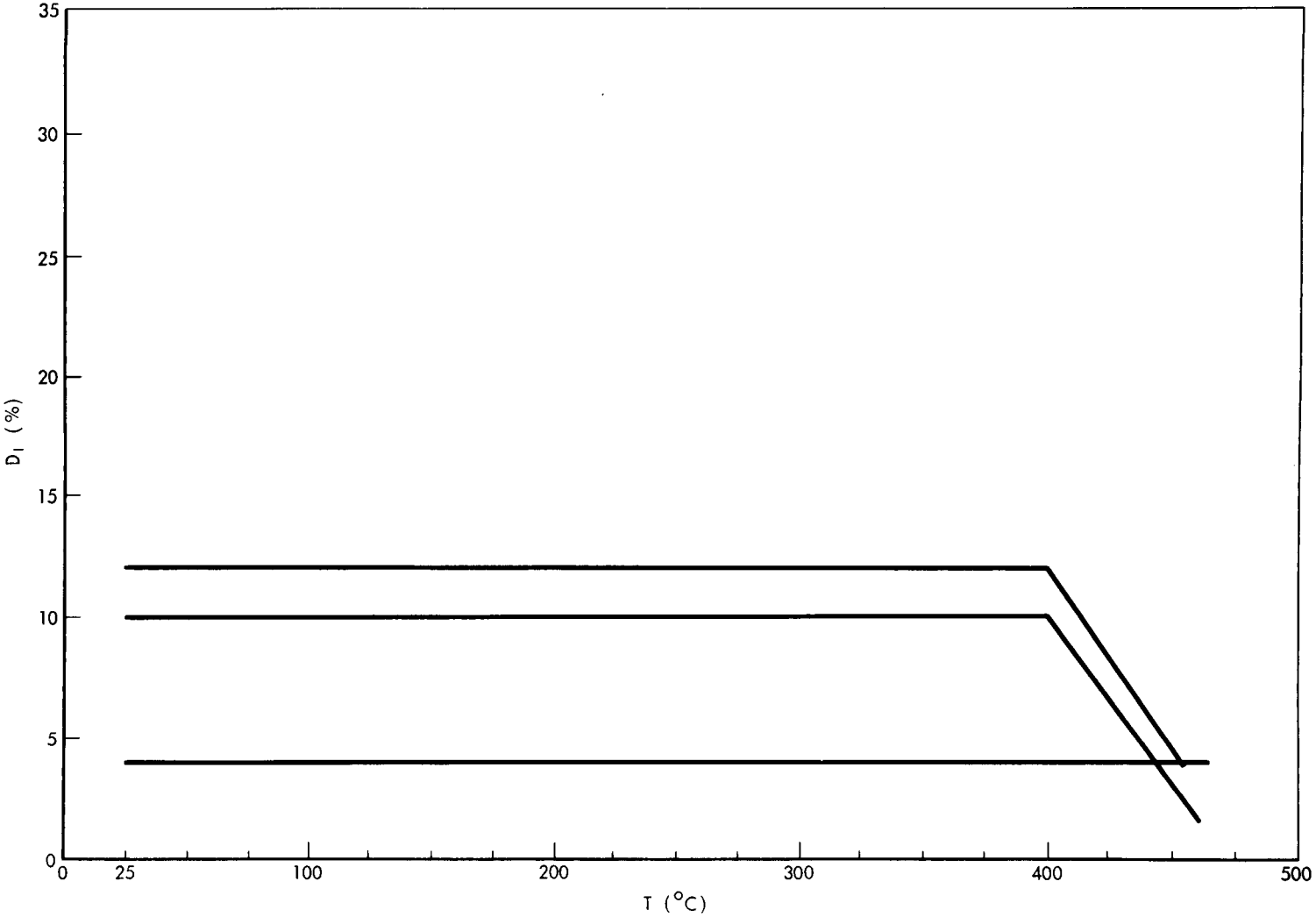

Figure VIII-1. Annealing Characteristics of P and N Solar Cells of 1Ω cm Base Resistivity, with Different Initial Stage of Damages

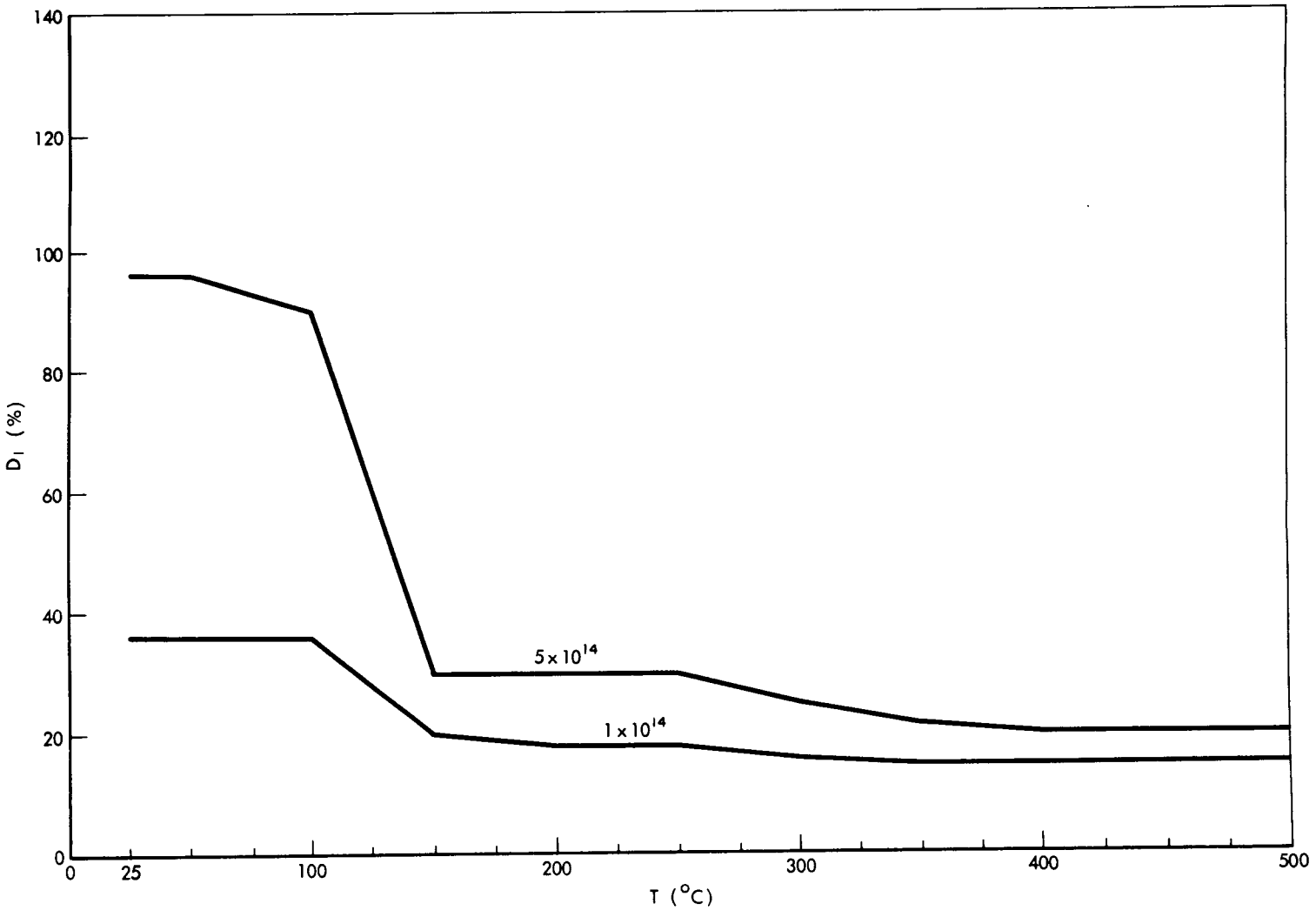

Figure VIII-2. Annealing Characteristics of P and N Solar Cells of 37Ω cm Base Resistivity with Different Initial Stage of Damages

IX. ANNEALING OF HIGH ENERGY ELECTRON RADIATION DAMAGE

In order to investigate the energy dependence of the annealing characteristics of solar cells, a group of solar cells was irradiated with 30 Mev electrons from a linear accelerator*. The solar cells were 10 Ω-cm, as in most experiments. The results of isochronal annealing of cells with different flux levels are given in Figure IX-1. When the flux level is up to 2.8×10^{13} e/cm^2, the annealing is complete at 400° C. There is a data gap at present between 2.8×10^{13} and 2.7×10^{14} e/cm^2. At 2.7×10^{14}, e/cm^2 unannealable damage is observed. However, owing to the above noted data gap, this value may be high. Compared with 1 Mev data of Figure V-2, where unannealable damage occurs near 1×10^{15} e/cm^2, this value indicates that the completeness of solar cell annealing at high energy is in general agreement with the energy dependence of the number of defects produced as measured by Carter and Downing (Reference 1).

Figure IX-1 also contains two isochronal annealing curves for 1 Mev electron irradiation with a damage level approximately that of a 30 Mev, 2.7×10^{14} e/cm^2 curve. In the high temperature region (above 300° C), the 1 Mev and 30 Mev curves are quite similar. However, in the low temperature region, 30 Mev curve shows progressive low temperature recovery. This can be explained by the following process:

---

*With the kind help of Dr.V.A. Van Lint of General Atomic, San Diego, California.

The damage introduced by 1 Mev radiation is highly attenuated near the base region, and the damage of 30 Mev radiation is more uniform throughout the solar cell, but exists in both the surface N-layer and the bulk P-layer. This results in a quantum yield spectrum as shown in Figure IX-2. Comparing Figure IX-2 with Figure IV-2, 30 Mev radiation produces more damage in the short-wavelength region (below 0.55μ) than 1 Mev radiation. Annealing in this region is easier for two reasons:

1. The dominant contribution of quantum yield in this region is from N-type silicon which has an E-center defect due to the radiation, but this defect can be annealed near 200° C (see Chapter VII).

2. According to the recent work of Bemski (Reference 2), defects near the surface can be more easily annealed.

REFERENCES

1. Carter, J.R. and R.G. Downing, Changed Visible Radiation Damage in Silicon, XI. Contract No. NAS5-3805.

2. Bemski, G. and C.A. Dias, J. Appl. Phys. 35, 2983 (1964).

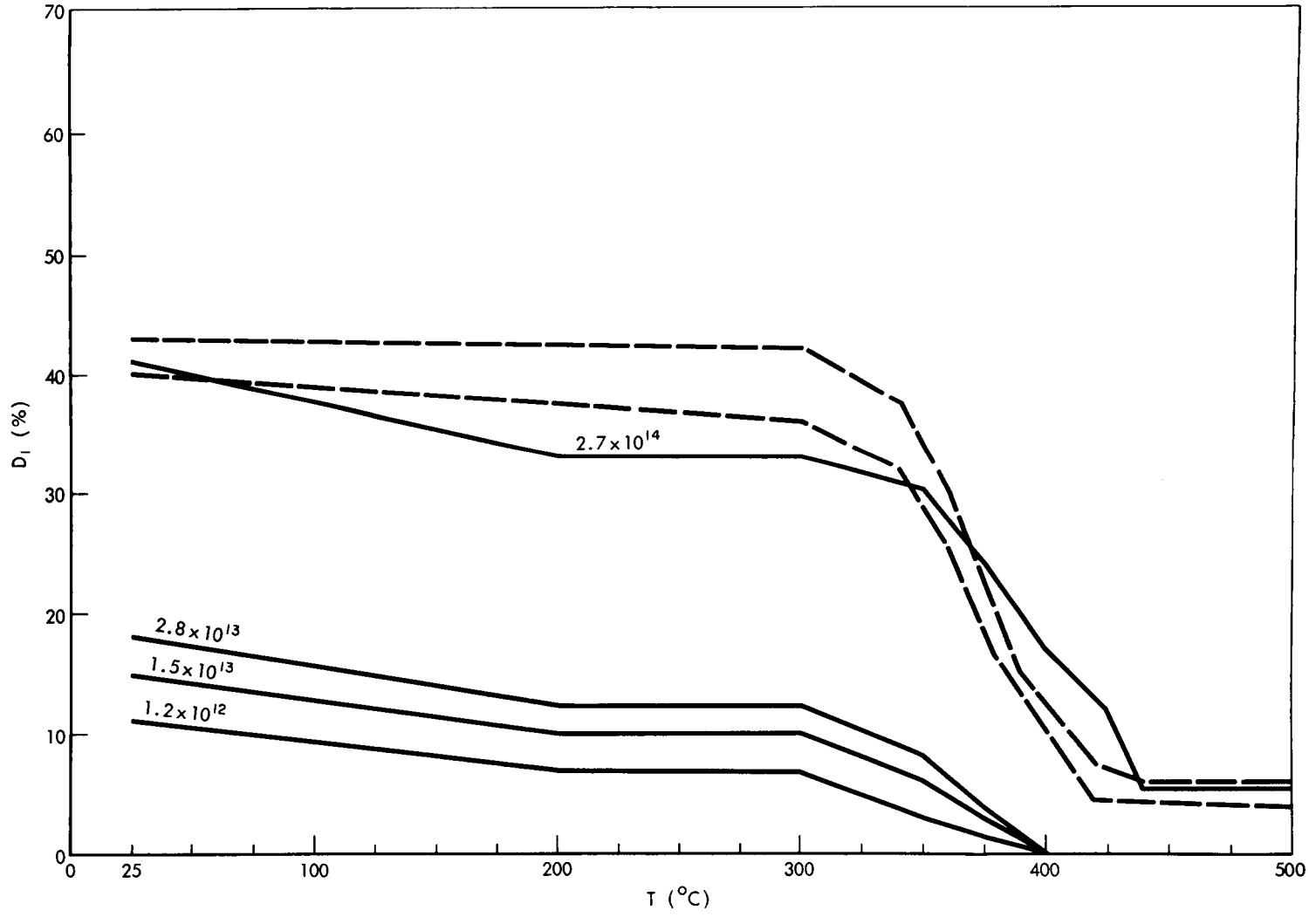

Figure IX-1. Isothermal Annealing of 1Ω cm Solar Cells with 30 Mev (Solid Curves) and 1 Mev (Dotted Curves) Radiation at Different Flux Levels

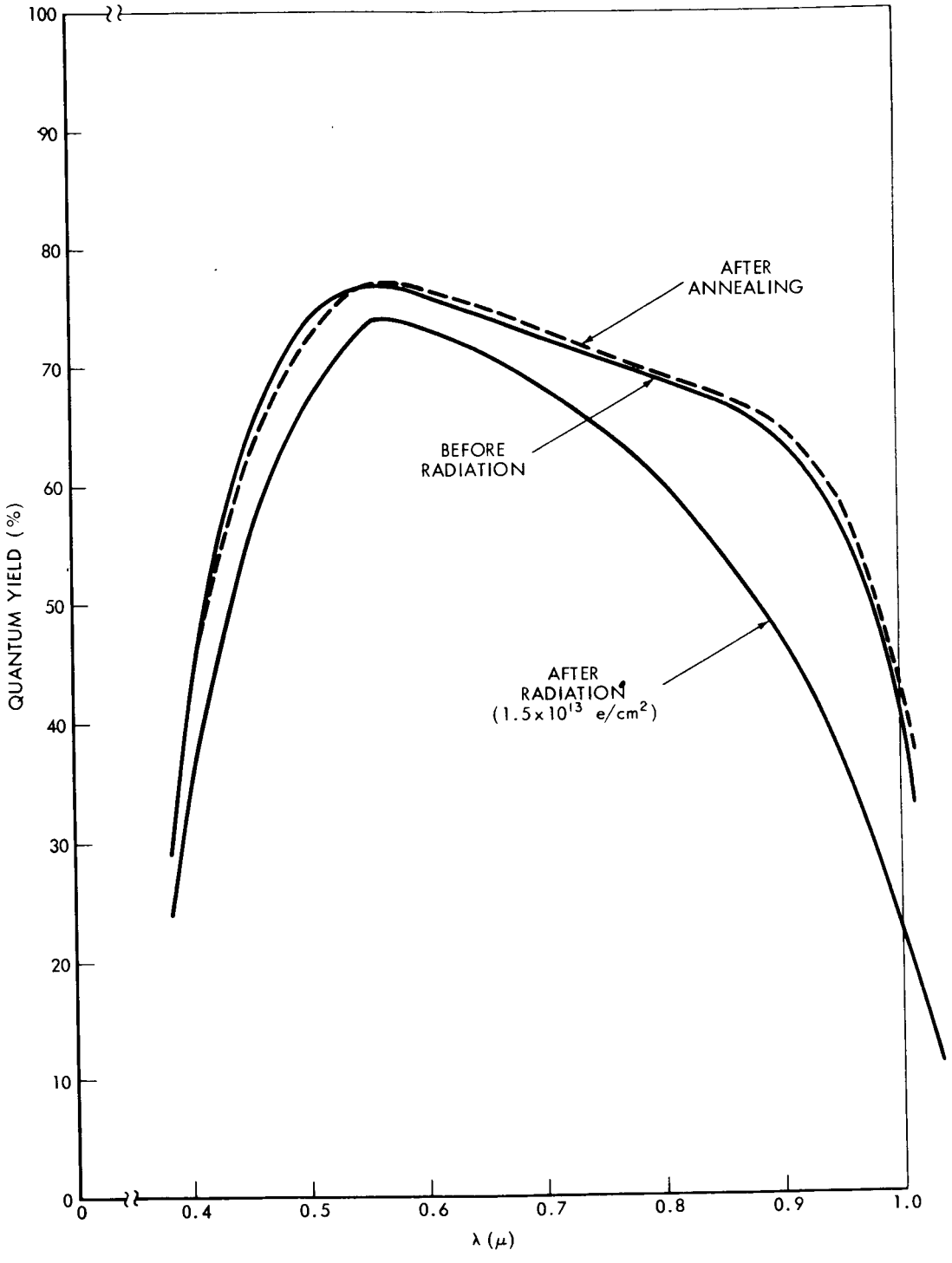

Figure IX-2. Spectrum of Quantum Yield for 30 Mev Radiation and Annealing of a 10Ωcm Solar Cell

X. ANNEALING OF PROTON RADIATION DAMAGE

The characteristics of proton damage are:

1. The energy-range relation is more sharply defined than in the case of electron damage.
2. For a low-energy proton (1 Mev), the damage increases rapidly as E^{-1} increases.

Although the first characteristic relation can be conjectured from the theory of Seitz-Koehler (Reference 1), the mechanism required to produce the second characteristic is not well known. Our study of annealing reveals some properties of low-energy damage.

All the solar cells used are similar to those described in Chapter III. The energies of radiation are 0.10, 0.30, and 0.45 Mev protons. Figure X-1 shows a spectral response of 0.10 Mev radiation. The flux is 6.25×10^{11} p/cm^2. A dominant damage is in the blue region of the spectrum, and unannealable damage occurs at wavelengths greater than 0.74μ. At this wavelength, the optical absorption is 1.5×10^3 cm^{-1} (Reference 2) and the reciprocal value is 6.7μ. On the other hand, the range-energy relation gives a penetration depth of about 1μ for a 0.10 Mev proton. Therefore, the damage is not restricted to the N-layer. The damage to the effectiveness of the junction has yet to be studied. Figure X-1 also shows that a 200°C annealing for 15 minutes shows negligible effect, thus negligible E-center contribution to the damage.

Figure X-2 shows the results of the same energy protons as Figure X-1, but at the higher radiation flux level of 5×10^{12} p/cm^2. An increase in the bulk damage is evidenced from the long wavelength region of the spectrum. We also observed increased annealability. The isochronal annealing curve for this case is shown in Figure X-3. A large annealing stage occurs between 100° to 200°C and a simple scheme to explain this observation would be an annealing of E-centers. This would be consistent with the picture of dominant top layer damage as this layer is of N-type. However, it fails to explain an absence of an annealing effect at high temperature, in spite of the fact that an initial, noticeable annealing also occurs in the long wavelength region. According to the previous results of electron radiation, damage in the long wavelength region can be annealed unless the radiation flux exceeds a threshold value. It appears at present that the unannealable damage in the long wave region is indeed of the type discussed in Chapter VI. More work is needed to verify this mechanism.

Figure X-4 shows the spectral response of 0.30 Mev radiation and two isothermal annealing curves with 5 and 15 minutes annealing at 200° C. Isochronal annealings for two flux levels of radiation are shown in Figure X-5. A gradual decrease of the radiation damage in the long wavelength region of the spectra is reflected in the efficient annealing shown by the isochronal curves. A noticeable increase in the effect of 100° to 200°C annealing is observed in the case of high radiation flux levels.

Figures X-6 and X-7 are for 0.45 Mev radiation. The general trend of change from 0.30 Mev radiation follows that of a gradual change from 0.10 to 0.30 Mev radiation. The annealing in X-6 was for 5 minutes at 200°C. No No additional annealing was observed after an additional 10 minutes of heating.

In future analysis, we hope to discern two effects:

1. From the dark I-V curve, the degree of damage to the junction.

2. According to the results presented in Chapter V concerning the dependence of radiation damage and annealing on the resistivity of solar cells, we suspect a more severe proportion of unannealable damage in the N-region. This is because there is a very large concentration of donor impurity which converts the P-type substrata of silicon to a compensated layer (N-P junction) and further into an N-type surface.

There is an appreciable, although not always systematic, annealing even at room temperature (Reference 3). This points to two possible—and not necessarily mutually exclusive— types of effects. The first effect, speculated on in Chapter IV, is a large cluster of defects, with a size of 10 lattice constants, but with the same type of defect structure (such as A- or C-centers) as was observed in the EPR work of Watkins (Reference 4). The second type is a thermal damage as theoretically speculated on by Brinkman (Reference 5) and Smivnor (Reference 6). The indirect experimental observation of Bemski and Dias (Reference 7) may be this type. Bemski and Dias observed an efficient

room-temperature annealing of defects thermally quenched-in from 870° to 1070° K. A thermal defect could have a much larger dimension, say 10^3 lattice constant, and may be related to the defects directly observed by Bertolatie.

From a practical point of view, we have to conclude that in the case of proton damage complete annealing as in the case of electron damage cannot be expected. Fortunately, recent progress with integrated solar cells with a deposited glass cover (Reference 8), instead of the usual type of solar cell with a glass cover bound on with an adhesive (which would restrict the annealing temperature), should help to minimize proton damage while permitting an effective annealing of electron damage. The investigation of annealing of integrated solar cells with both electron and proton radiation is in progress.

REFERENCES

1. Seitz, F. and J. S. Koehler, Solid State Physics, Vol. 2, edited by F. Seitz and D. Turnbull (Academic Press), 1956.
2. Dash, W. C. and R. Newman, Phys. Rev. 99, 1151 (1955).
3. Downing, R. G., (Private Communication).
4. Watkins, G., 7th International Conference on Radiation Damage in Semiconductors (Dunod, Paris 1965) p. 97.
5. Brinkman, J., J. Appl. Phys. 25, 961 (1954).
6. Smivnov, L. S., Fiz. Tverd. Tela. 2, 1669 (1960).
7. Bemski, G. and C. A. Dias, J. Appl. Phys. 35, 2983 (1964).
8. Iles, P. (Private Communication).

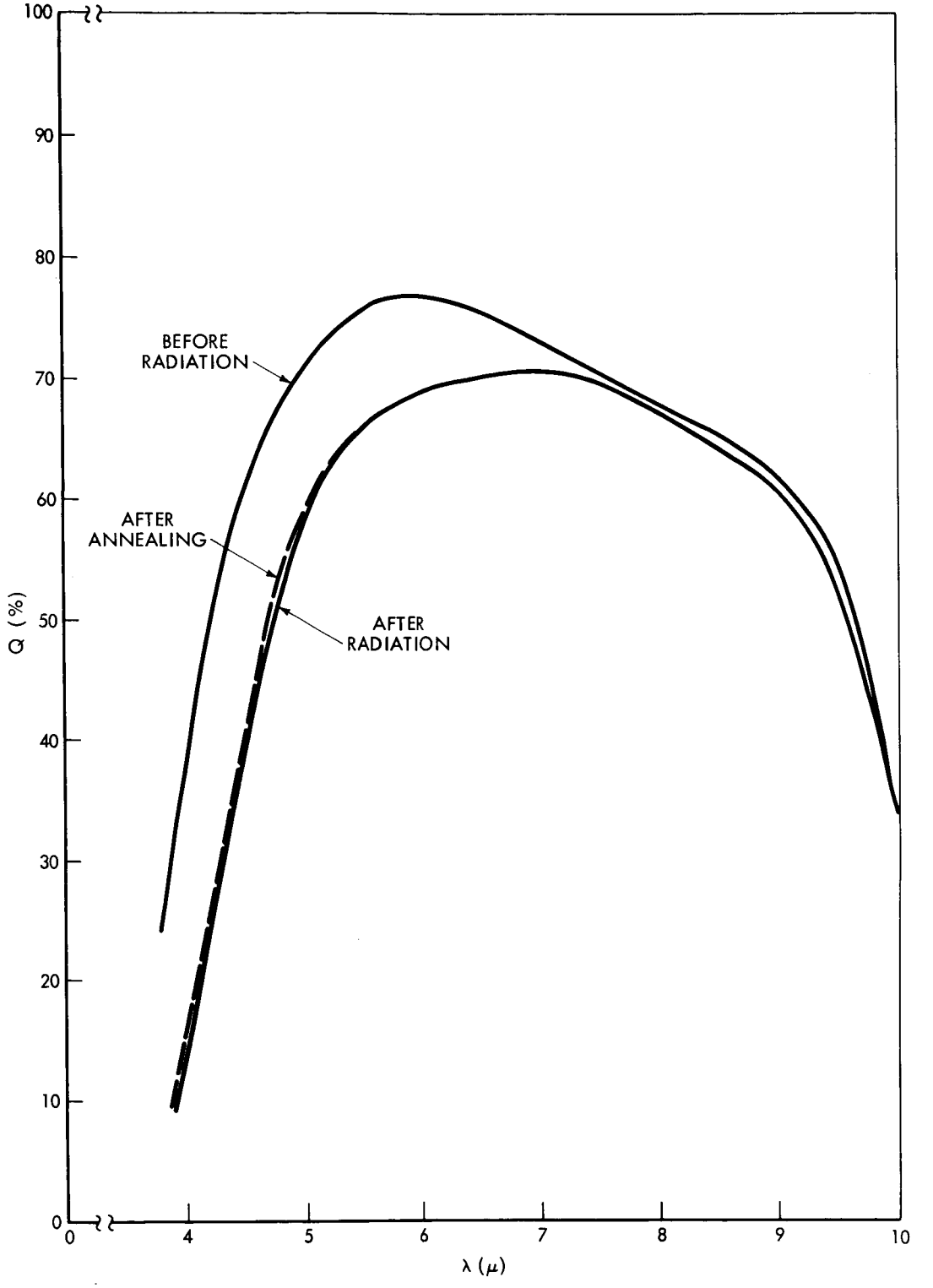

Figure X-1. Spectral Response of Solar Cells with 0.1 Mev 6.25×10^{11} Proton/cm Radiation and Annealing

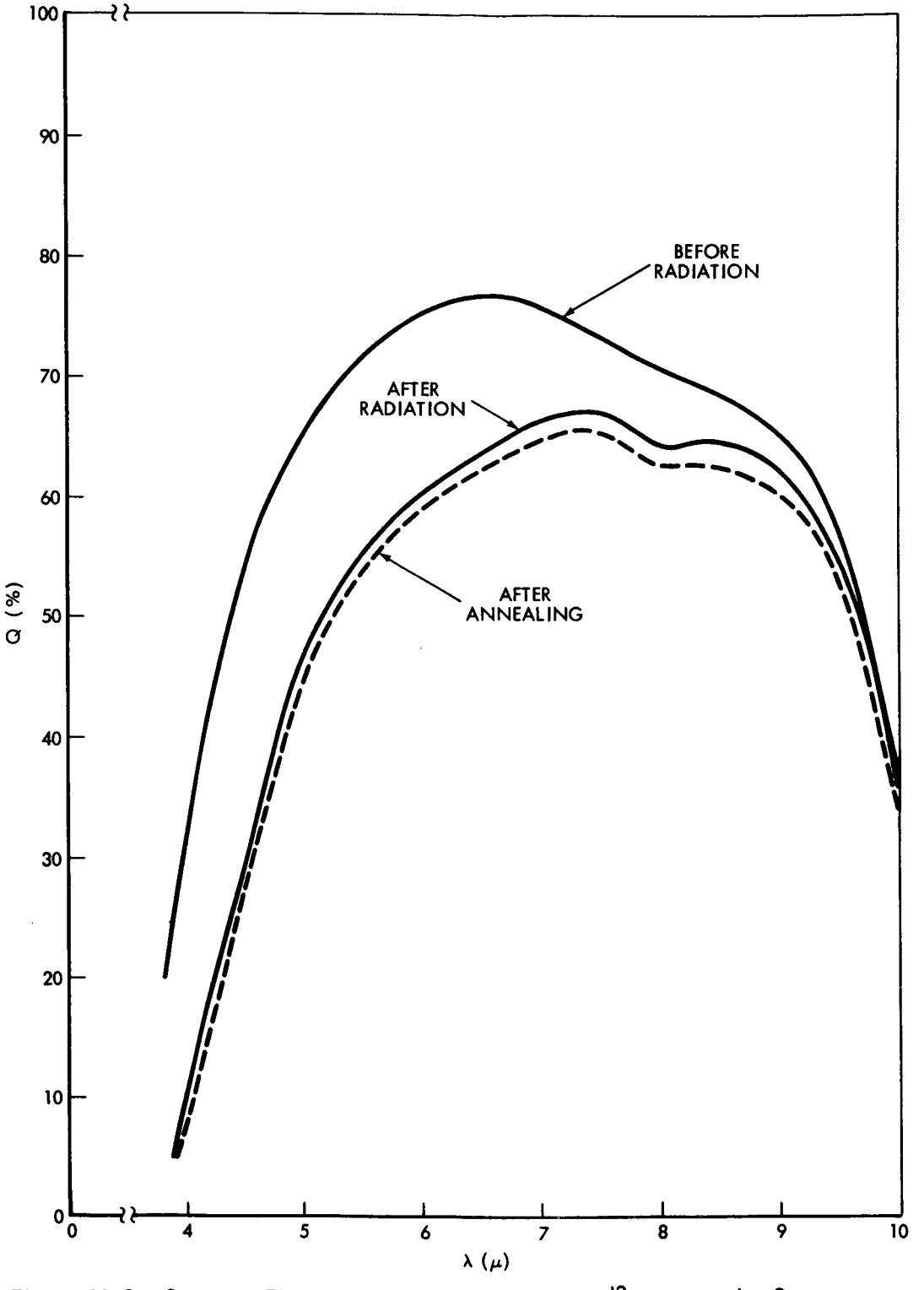

Figure X-2. Same as Figure X-1 except with 5×10^{12} Protons/cm^2 Radiation

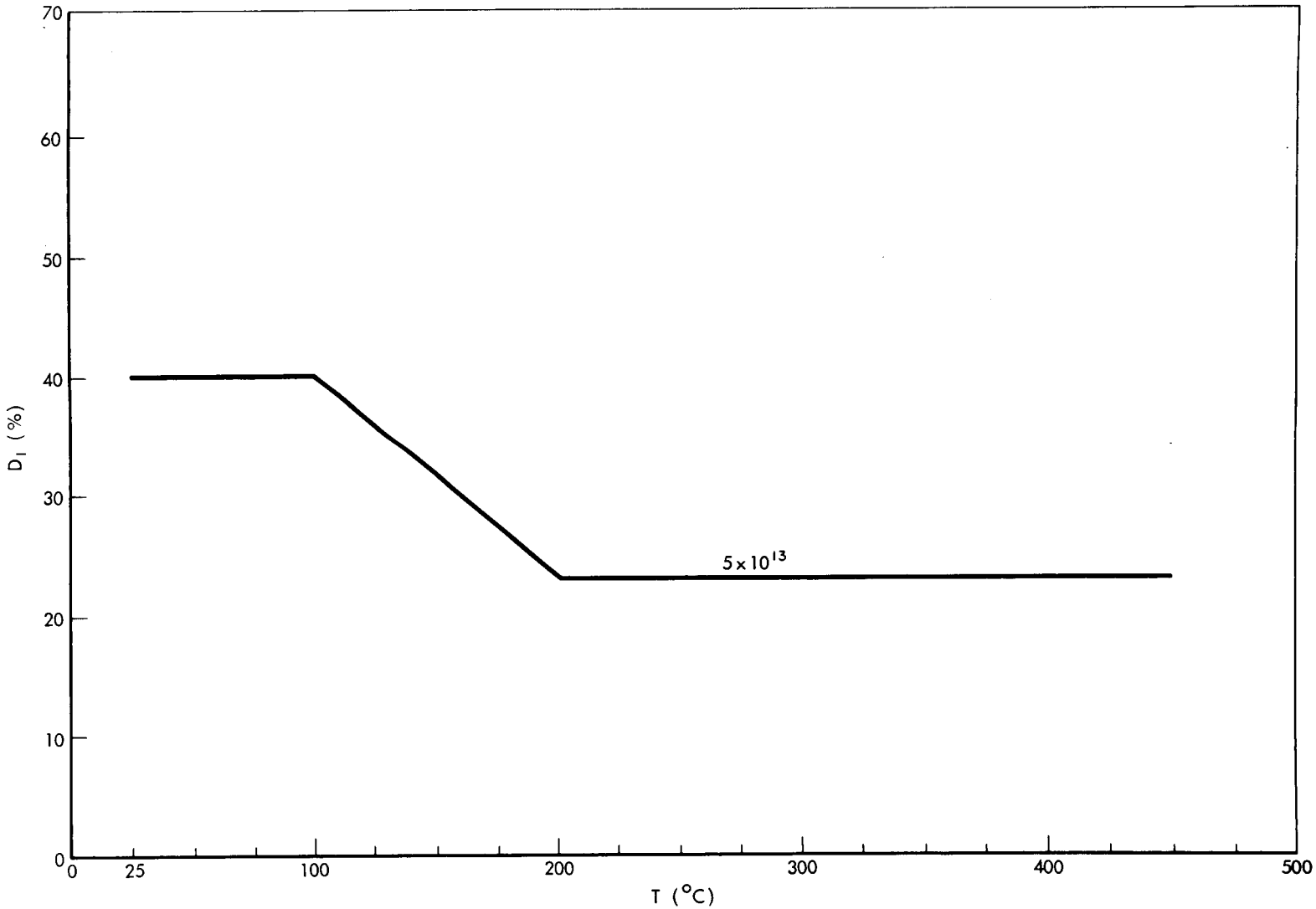

Figure X-3. Isochronal Annealing from the Specimen of Figure X-2

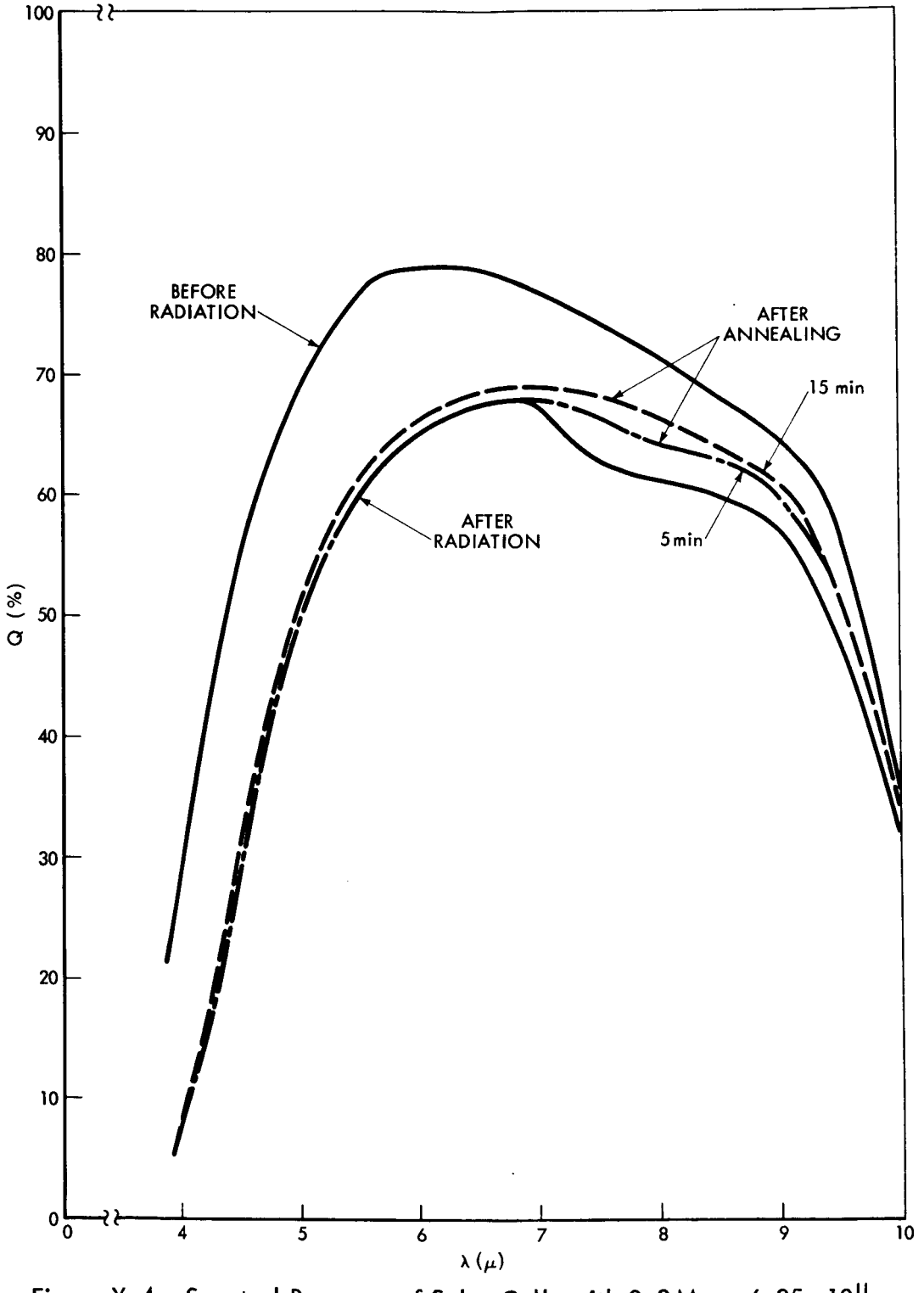

Figure X-4. Spectral Response of Solar Cells with 0.3 Mev, 6.25×10^{11} Protons/cm² Radiation and Annealing

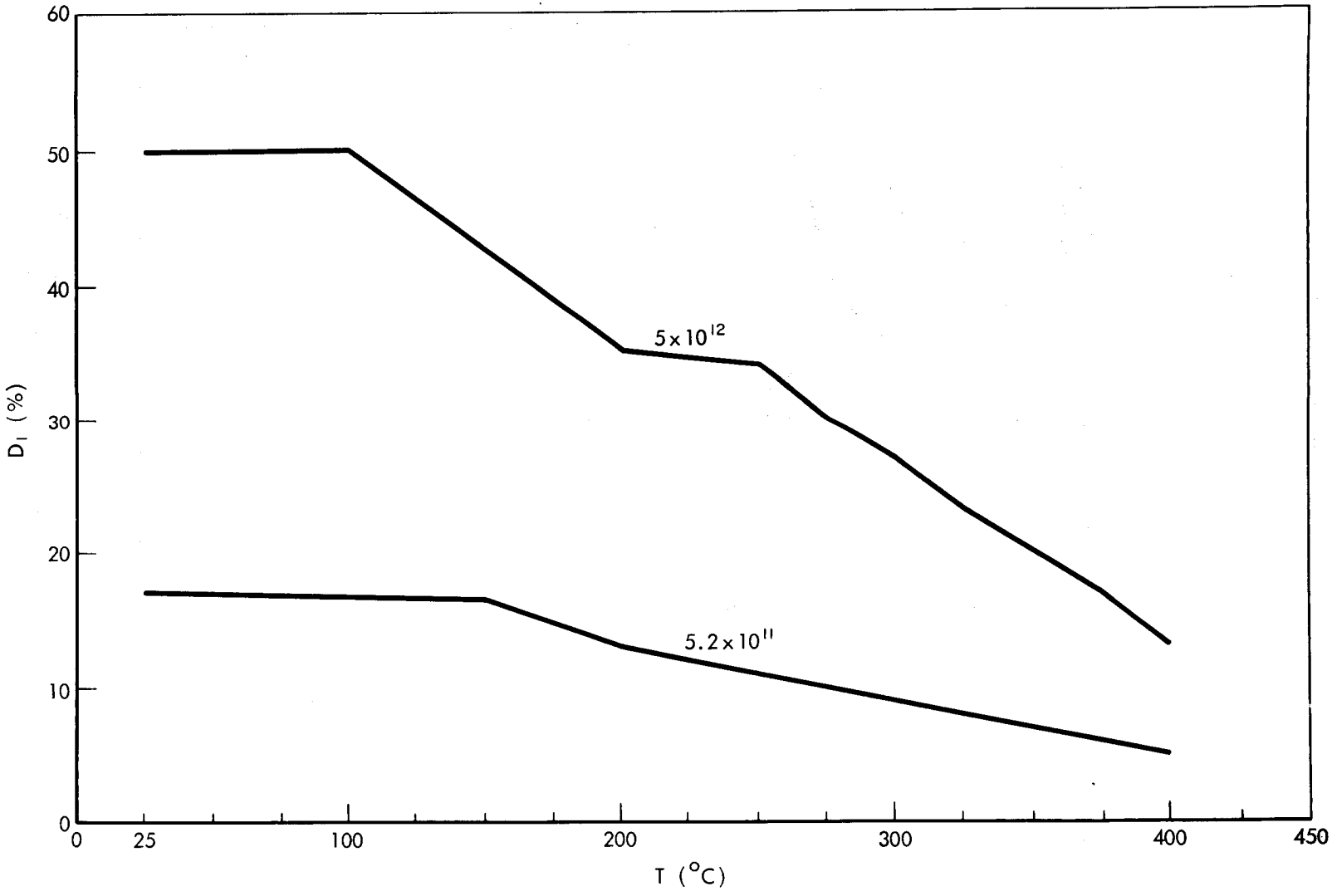

Figure X-5. Isochronal Annealing for 0.3 Mev Proton Radiation

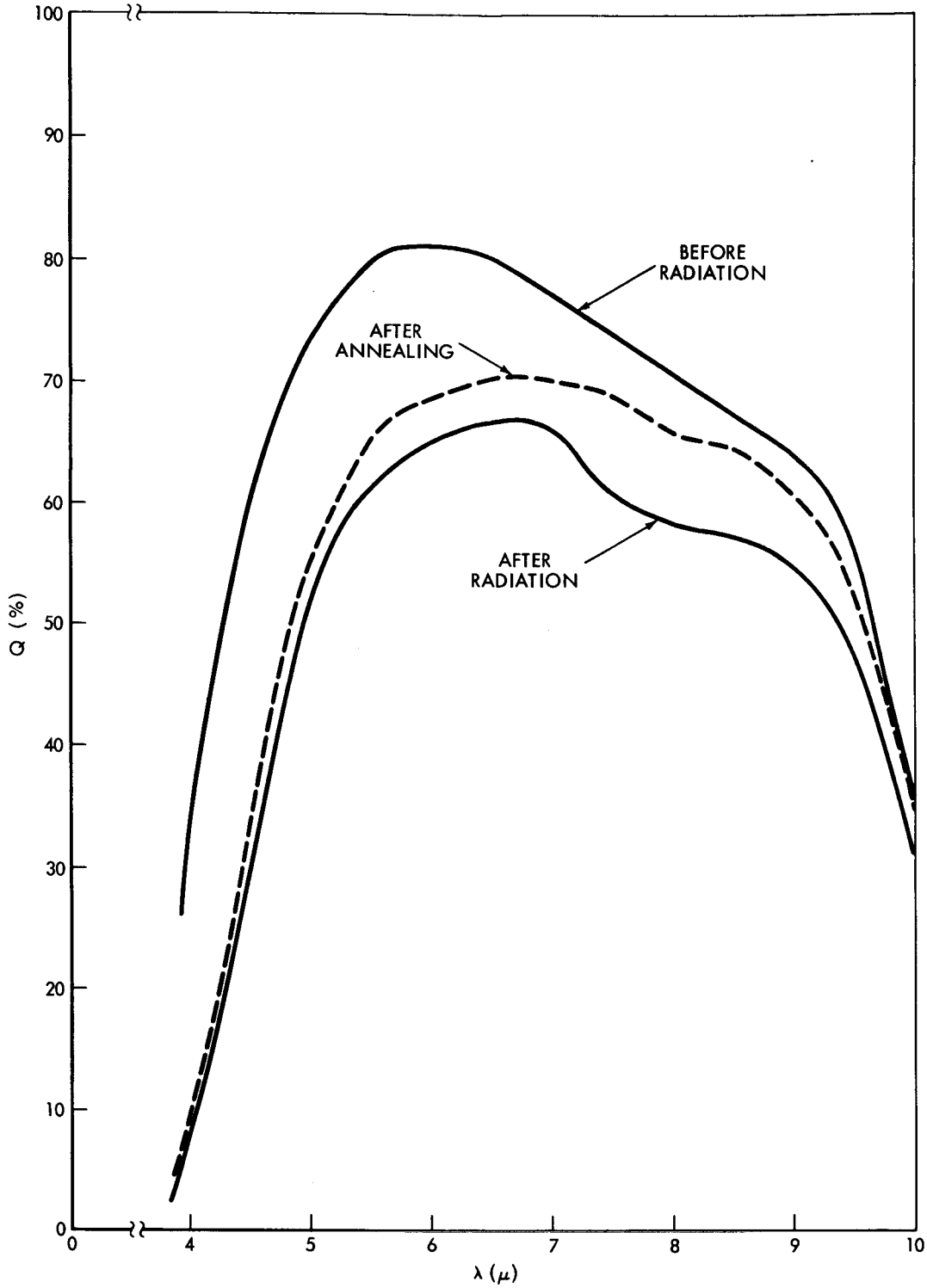

Figure X-6. Spectral Response of Solar Cells with 0.45 Mev, 9×10^{11} Proton/cm^2 Radiation and Annealing

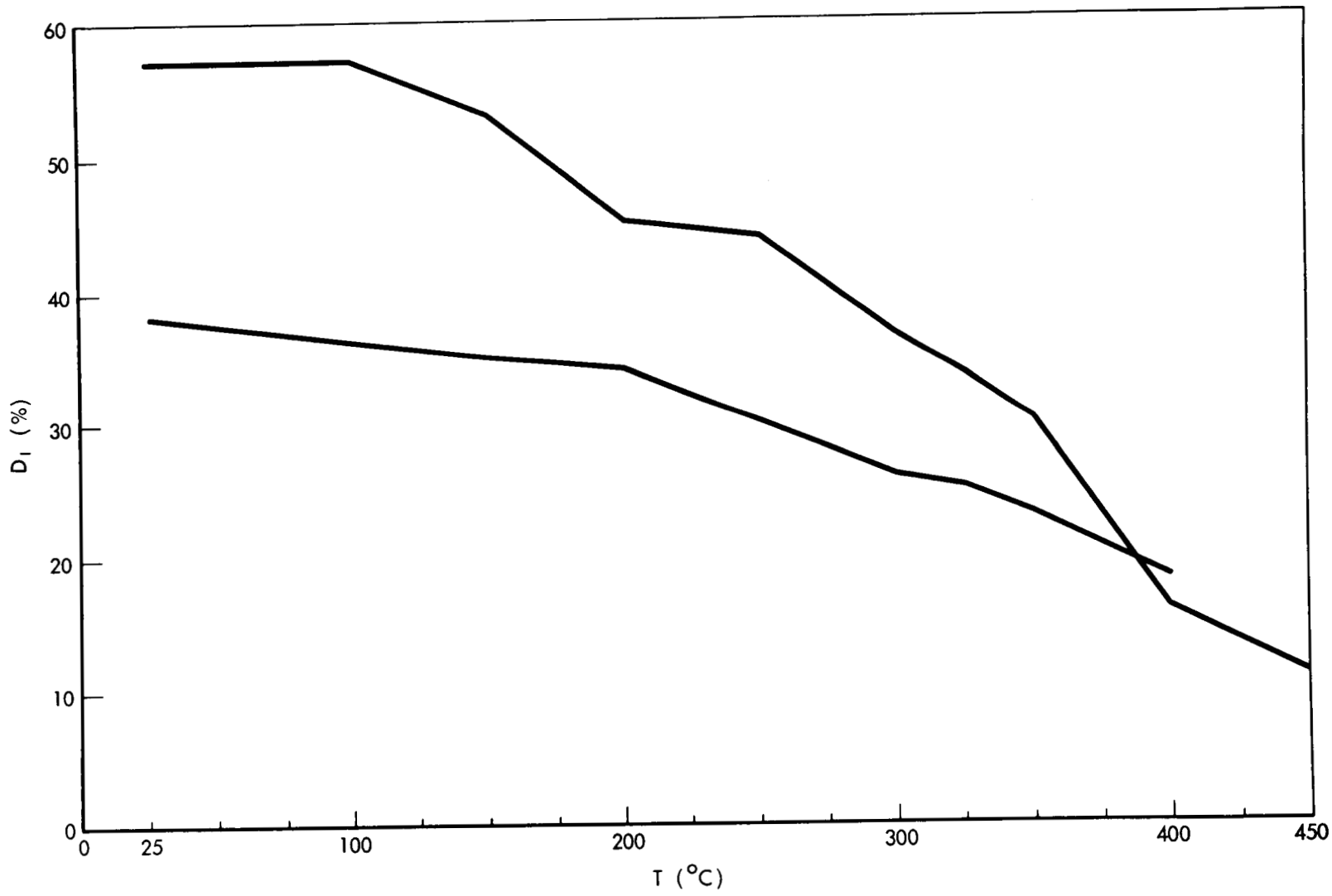

Figure X-7. Isochronal Annealing of 0.45 Mev Proton Radiation

XI. TEMPERATURE DEPENDENCE OF RADIATION DAMAGE

Radiation with 1 Mev electrons was carried out with the specimen kept at 22° or -196°C. There was a slight increase of about 2°C during the radiation in both cases. A difference in degree of damage in these two radiation experiments was observed: A greater degree of damage was observed in the case of the higher temperature irradiation. This effect diminishes for a very large radiation flux. A most obvious effect was to the characteristics of reverse annealing which will be described below.

Isochronal annealing was carried out with identical treatment to the specimen irradiated at different temperatures or with different fluxes. The results are shown in Figure XI-1. As can be seen from the figure, in general, the damage measured at 22°C is higher in the case of radiation at 22°C than that at -196°C.

There is a reverse annealing stage above 150°C. This stage is much less evident for -196°C radiation than the case of 22°C radiation, and indicates the defect responsible for the reverse annealing is produced efficiently only when radiation is carried out at a sufficiently high temperature.

In a further study of this reverse annealing, we observed that if we omit the 100° and 150°C isochronal annealing stage and initiate the annealing at 175°C and increase the temperature in 25°C steps thereafter, no reverse annealing

was observed. Consequently, we did not observe a reverse annealing in isochronal measurements carried out near 200°C. Therefore, the activation energy of this reverse annealing cannot be determined.

The reverse annealing observed in the present work occurs in the same temperature range and behaves similarly to that observed by Inuishi et al.[2] Two alternative interpretations are possible. Assume the reverse annealing is a manifestation of a dissociation of simple A-center as suggested by Inuishi et al. The complete annealing in the present case occurs near 400°C, which on the other hand, the reverse annealing is completed near 250°C. The vacancy dissociated from the A-center should anneal very near to 250°C in this case. The consequence of this interpretation is that the dominant high temperature annealing stage near 400°C could not be the A-center, but the J-center, which is a divacancy in p-type Silicon.[3] However, this interpretation does not explain the temperature dependence we observed in the present work.

An alternative explanation is the following. The reverse annealing is a dissociation of a small, lightly bound cluster of defects. The formation of the cluster would depend on the concentration of the defect centers, and therefore, would depend on the temperature of the specimen during the radiation. It may be noted that photovoltaic measurement provides a possibility for studying the dependence of the production of a defect on the concentration of other defects. In

EPR or optical studies of defect production, the radiation flux level is usually so high that the concentration effect is saturated.

REFERENCES

1. P. H. Fang, Phys. Letters 16, 216 (1965)
2. Y. Inuishi and K. Matsuura, J. Phys. Soc. Japan 18 (Suppl. III) 240 (1963)
   T. Tanaka and Y. Inuishi, ibid. 19, 167 (1964)
3. R. R. Hasiguti and S. Ishino, Symposium on Radiation Damage in Semiconductors (Dunod, Paris, (1965) p. 209

LIST OF FIGURES

Figure 1 – Isochronal annealing of Silicon, ⊙, specimen at -196°C during the radiation; △, specimen at 22°C during the radiation. (The marks near the curves represent the total number of 1 Mev e/cm^2).

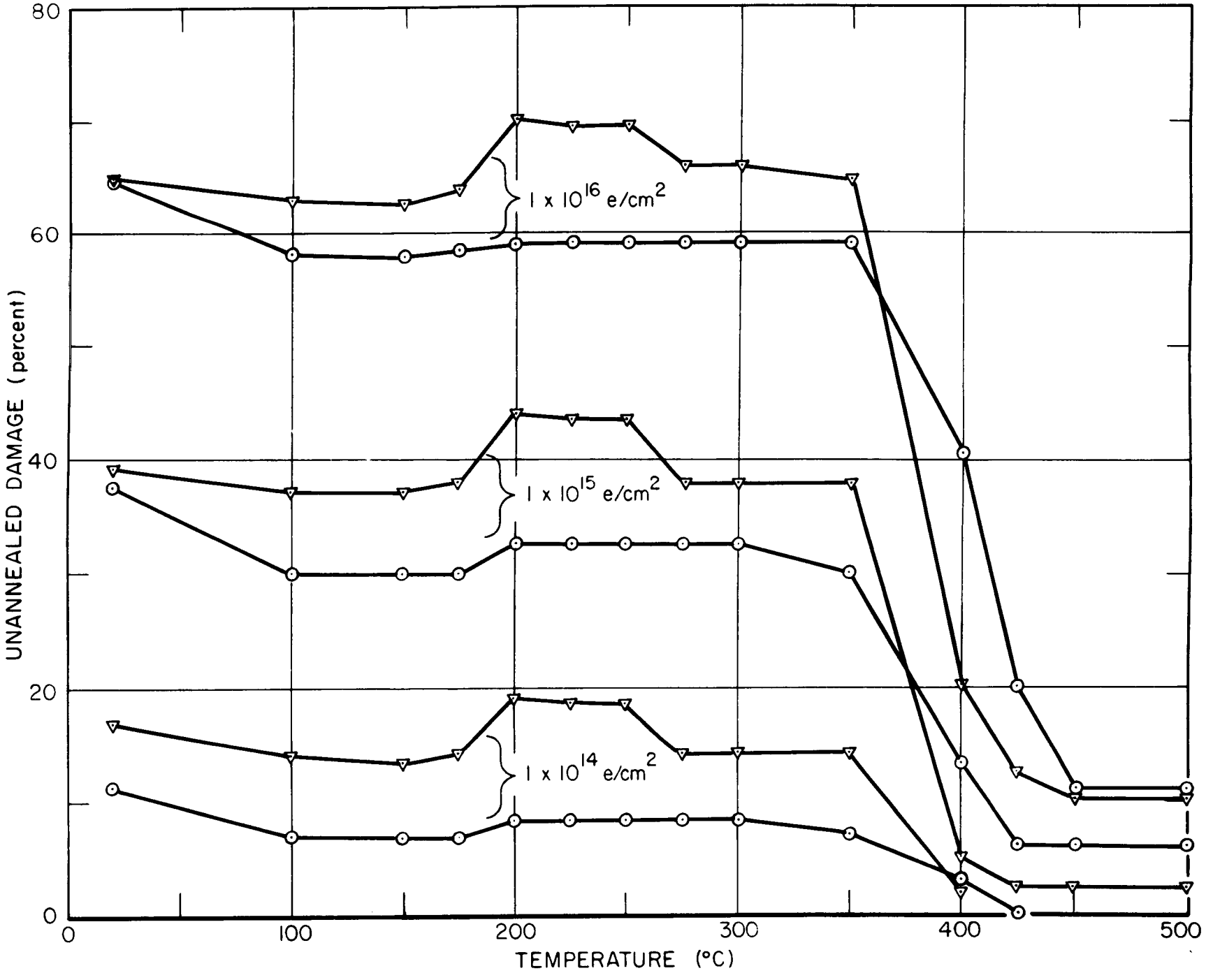
80
60
40
20
0
0
100
200
300
400
500
UNANNEALED DAMAGE (percent)
TEMPERATURE (°C)
1 x 10^16 e/cm^2
1 x 10^15 e/cm^2
1 x 10^14 e/cm^2

Figure XI-1

XII. THERMAL SYSTEMS FOR ANNEALING

The method which will be presented here is more for an investigation of the principle and feasibility than an actual engineering design.

There are two fundamental problems:

1. The thermal source for annealing; and
2. The machinery to transfer the heat for annealing.

An estimation of the required heat was made by Mr. N. Ackerman of the Temperature Control Section of the Thermal Systems Branch. Assuming a black body radiation heat loss into 0°K surroundings, the necessary heat to maintain a 400°C temperature is about 300 watts/ft^2 of a solar panel, which is approximately 0.67 watt/2 cm^2, 2 cm^2 being the surface area of the ordinary solar cell. This is to be compared with the power output of about 0.02 watt/2 cm^2 from an ordinary solar cell.

A great improvement is obtained by covering the solar panel during anneal with polished surfaces. If two closely adjacent, but not contiguous, surfaces are used, the required power is reduced to 27 watt/ft^2 or equivalently, 0.03 watt/2 cm^2. Therefore, the power required to anneal one solar panel can be supplied by about one and one-half solar panels which are facing the sun and therefore in a state of power production. Such a system has been considered and will be discussed under Supplementary Heating System.

Two other approaches have been considered. The first is a chemical heat source and reaction chambers. This approach has been studied in some detail by Dr. B. Fabuss of the Monsanto Chemical Company (Reference 1). Because of the excessive weight and complicated machinery involved, this approach is unfavorable.

The second approach was suggested in principle by Professor J. Loferski of Brown University (Reference 2). The actual design was aided by discussions with Messrs. E. Power and S. Ollendorf of the Temperature Control Section of the Thermal Systems Branch.

The principle of this approach is to utilize the solar heat trapped by a "greenhouse effect." In this case, the solar panel is covered with a retractable window transparent to the visible and ultraviolet portion of the solar spectrum but opaque to the infrared.

The requirements of the window material are:

1. The material should be in the form of flexible sheet.
2. The material can stand the temperature in the vicinity of annealing temperatures, i.e., about 400° C.
3. The optical property of the material should be reasonably resistant to the space radiation and be stable in vacuum.

All these requirements are satisfied by the so-called H-film, a product of DuPont Chemical Company. My first contact with this material was on my visit to Dr. H. Jaffe of Clevite Corporation. He had used this film in the fabrication of film CdS film solar cells (Reference 3).

An optical coating on a large sheet of H-film was successfully carried out by Libby-Owens Ford Glass Company of Pittsburgh, Pa.

However, the second fundamental problem, as stated in the beginning (i.e., for a system to retract the window), discouraged a serious effort. In my conversation with Mr. W. Cherry of the Space Power Branch, he stressed the difficulty of moving parts in the space vacuum. The solution of this kind of problem is in sight, however, as is evident from the brushless DC motor developed by P. A. Studer of the Mechanical Systems Division (Reference 4). I understand now this is not the only motor capable of operation in a vacuum, but in early 1965, I had no knowledge of the existence of any other.

With the above information, a "solar panel" was constructed (Reference 5) to test the feasibility of our thermal system (Figure XII-1). A group of sixteen 2 x 2 cm^2 solar cells were attached to an aluminum panel of 1/8" thick 6 x 6" in dimension. A 1/2" shoulder was elevated on all four edges of the aluminum plate. All faces except the front surface were covered with a shiny aluminum film to reduce the heat radiation. The front surface was covered by the H-film with an

optical coating—the physical property of this film will be described later. Our purpose was to measure the heat obtainable; no motor-actuator system was used to place the cover film in position.

The system has two thermocouples. One was attached to the face near the solar cells. The temperature accuracy in this case was ±1°C. The other thermocouple is attached in the front surface of the H-film. The accuracy in this case probably was ±10°C.

The system is placed in a vacuum (Reference 6) of 1×10^{-6} mmHg. A carbon arc with the equivalent of one solar constant was used to illuminate the system. The time-temperature curve of this system is given in Figure XII-2. The notation coated or uncoated refers to the optical coating of the H-film, and an improvement of about 150°C is seen with the coated film. Thus with a coated film, after 1 hour, a temperature of 360° was obtained.

A temperature of 360°C is not quite sufficient to complete the annealing. One can take two alternatives. The first is to use supplementary heating. This has an advantage of providing better control of the annealing temperature.

A second alternative is to improve the "greenhouse effect" essentially through the optical properties. Figure XII-3 shows two transmission curves (Reference 7): H-film and H-film with coating. We immediately observe an opaque portion in the coated H-film, and this opaqueness is the intrinsic property

of H-film. We estimated that in the portion between 0.35 and 0.50μ, well over 30% of solar energy is distributed. In the whole solar spectrum, well over 50% of energy is not transmitted by the film. Therefore, an improvement in the transmission of H-film, or a replacement of this film by a more suitable film will be an important topic for investigation.

According to Figure XII-2, there is a difference of about 50° C between the solar cell and the window. The heating of the film is caused by the radiation of the solar cells and the absorption of the solar energy by the film. The absorption spectra of the film is given in Figure XII-4. As it can be seen, a large portion of the solar energy is absorbed by the film. If this portion can be reduced, the surface temperature can be decreased. In such a case even a film which cannot stand up to 400°C will still be suitable. We are investigating this at present.

Supplementary Heating System

Another simple heating system is to obtain ohmic heat directly from the solar cells by injecting a large current either through the grid and base connectors in a forward direction (Reference 8), or from one edge to the opposite of the base electrode. The base electrode, being a thin film, has a resistivity of the order of 0.1 Ω-cm. These two types of connectors have been constructed and tested at ambient atmosphere. The results are very satisfactory. The effects of utilizing the greenhouse effect and a supplementary heat system is to be studied in the future.

REFERENCES

1. Informal proposal from B. M. Fabuss of Monsanto Research Corporation, Everette, Mass., January 26, 1965.
2. Letter communication dated January 17, 1965. Later, in an informal proposal from E. Ralph of Heliobek (Dated July 2, 1965) a similar method was discussed.
3. Contract NAS7-20.
4. Goddard News, VIII, 8 (1965), P. Studer, NASA TN D-2108 (1964).
5. Promptly and economically constructed by Mr. G. Meszaros of our group.
6. This portion of the experiment was carried out at the facility of the Test and Evaluation Division, with the help of Mr. K. Rosette.
7. Kindly measured by J. Triolo's group of the Thermal Systems Branch.
8. There is evidence of deterioration of the junction by large reverse currents.

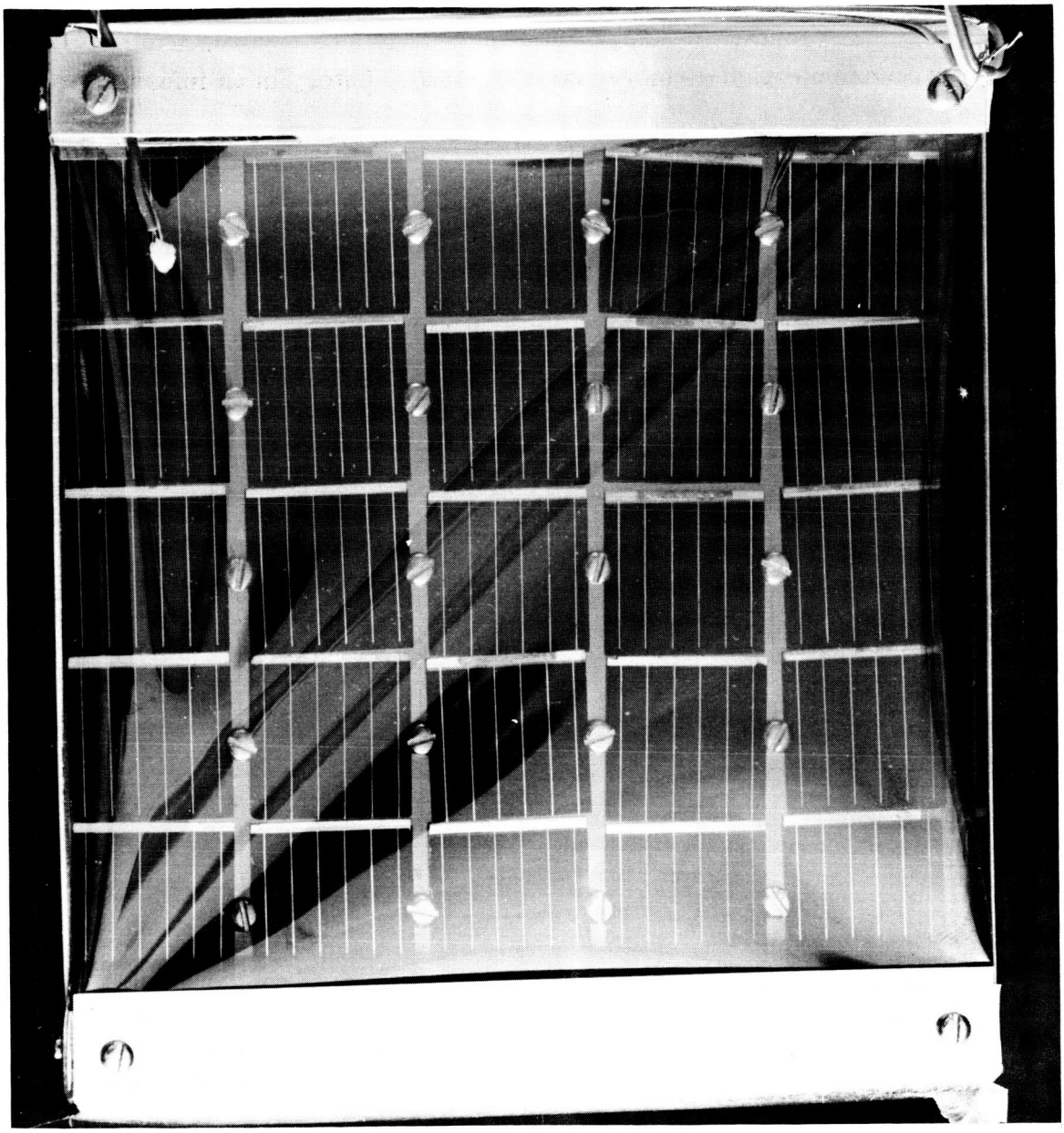

Figure XII-1. An Experimental Annealing Panel

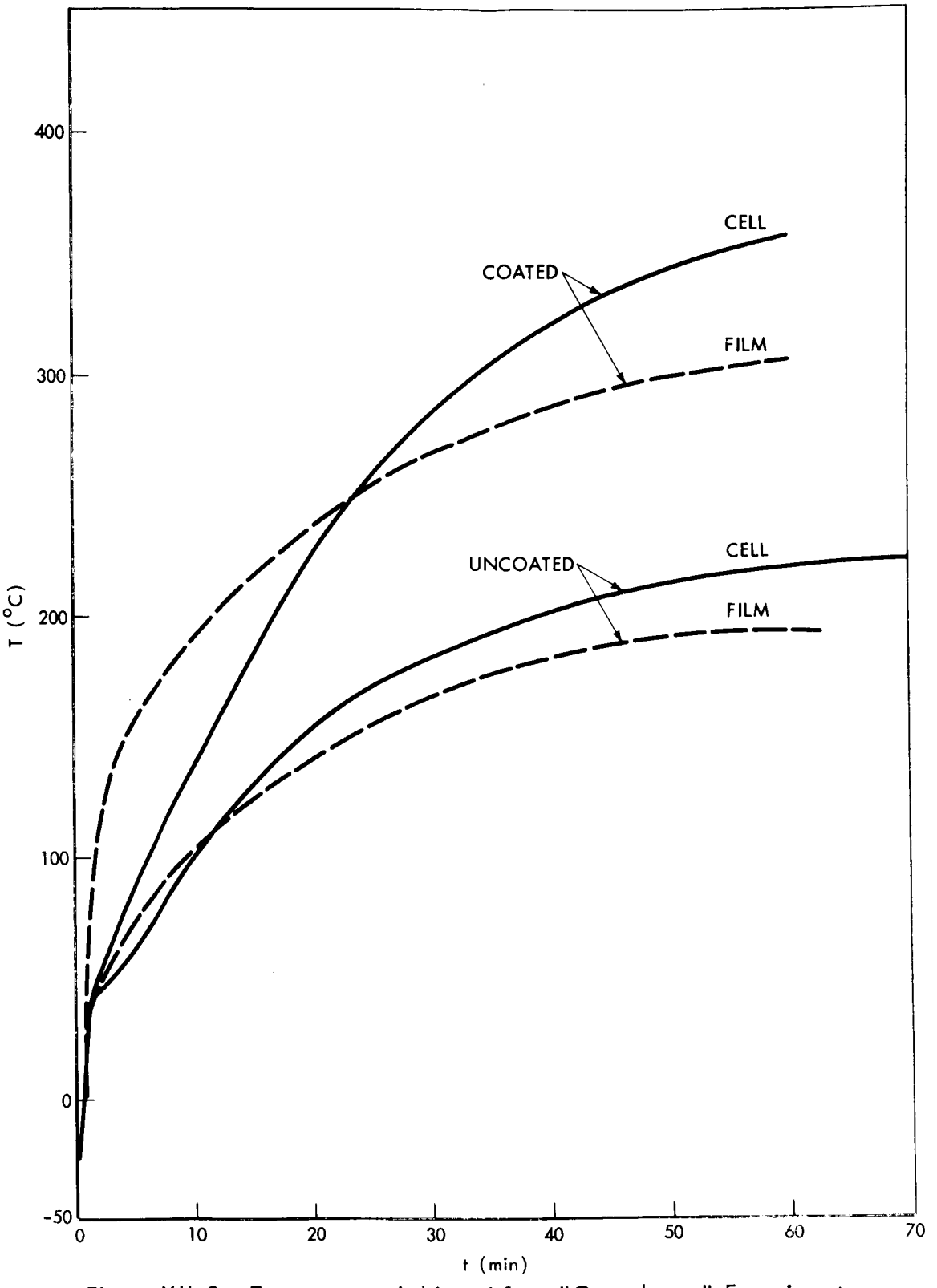

Figure XII-2. Temperature Achieved from "Greenhouse" Experiment

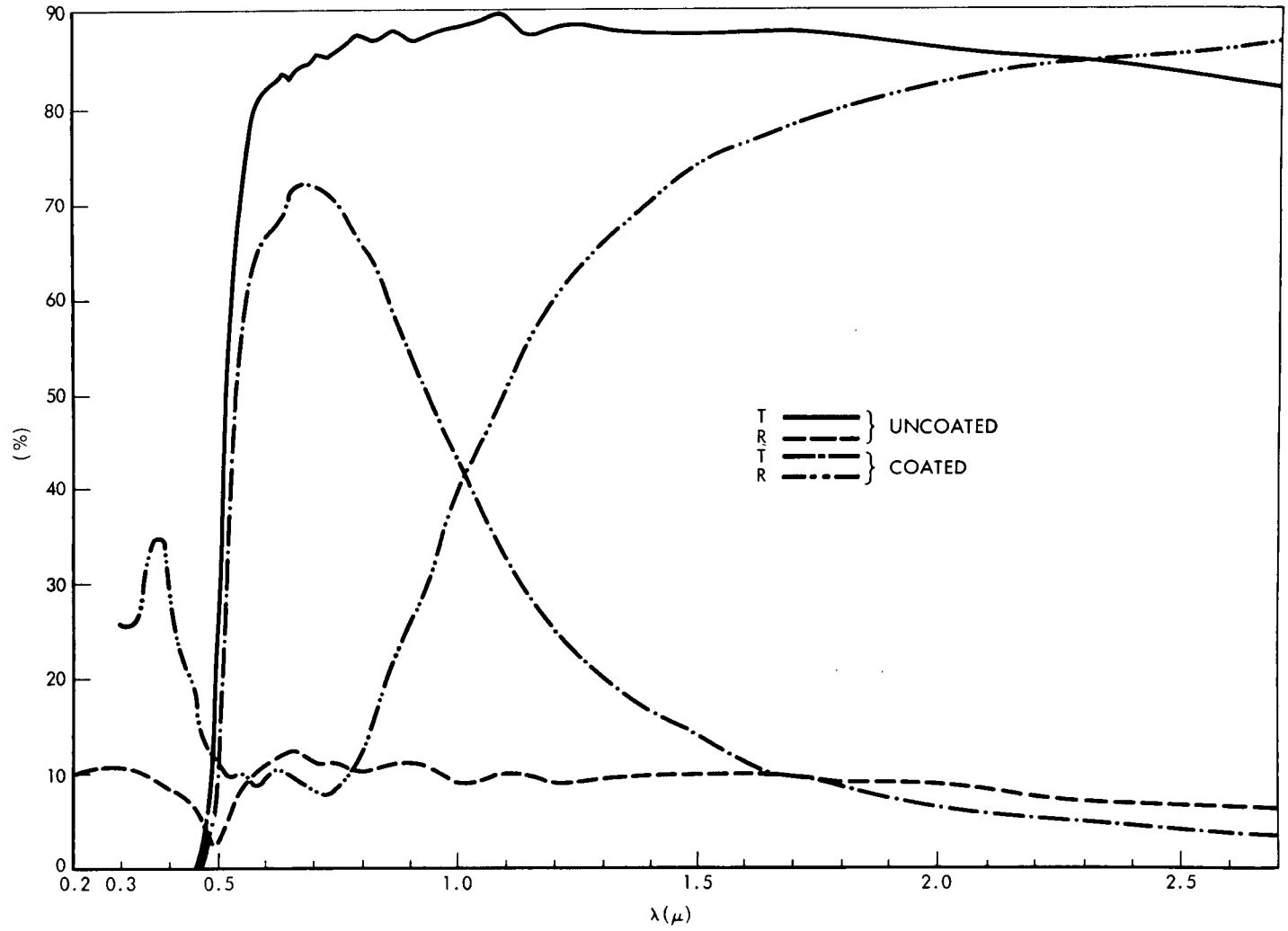

Figure XII-3. Optical Characteristics of H-film with and without Coating (T, Transmission, R, Reflection)

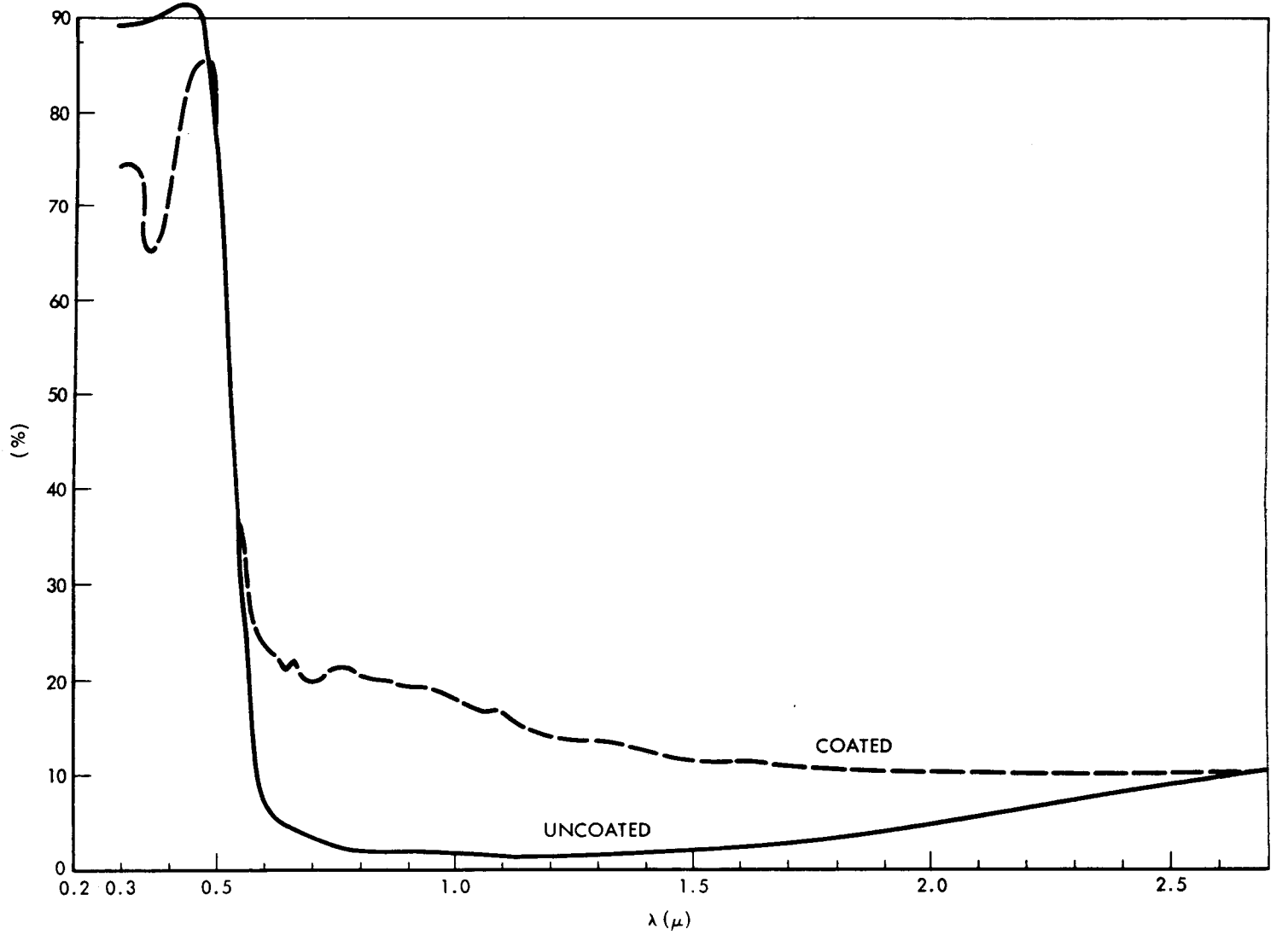

Figure XII-4. Absorption Characteristics of H-film with and without Coating

XIII. OUTLOOK

We have observed that damage due to electron irradiation can always be annealed independently of electron energy up to 30 Mev and presumably can be done so up to several hundred Mev. At very high energies, a spallation process could occur which would produce large clusters of defects which might profe difficult to anneal. There is no upper limit to the total flux as far as we can foresee, provided that intermediate annealing is carried out before the threshold of unannealable damage (as described in Chapter VI) is reached.

No experiments have been carried out with γ-radiation. But, based on our knowledge of the physical effects of γ-radiation on silicon, we expect that the annealing for this should be at least as effective as for electron irradiation.

In the case of proton damage, the annealing does not attain the same degree of completeness as in electron irradiation. However, for the most severe case of low energy proton irradiation (0.1 - 0.5 Mev), a 1 mil glass cover will provide adequate protection. Now, an integrated solar cell with a 1 mil glass shield has been developed by Hoffman Electronics. These cells have a nominal 10 percent efficiency. The glass cover has the same thermal coefficient of expansion as silicon up to 800° C—well above the required temperature for annealing. Therefore, in principle, proton damage should not present difficulties.

The system utilized in thermal annealing has been developed from currently available materials. We produced a greenhouse effect during annealing by covering the solar cells with a film which is transparent to visible light but opaque to infrared, thereby trapping the heat generated by absorption of solar energy. In this manner we have attained a temperature of 360° C, which is about 40° C below the required temperature for annealing. Some calculations have been made which indicate that with some improvements to the film coating, the required temperature can be reached.

In conclusion, there is no doubt that many new technological problems involving the solar cell panels have to be solved, and thus the task may appear quite formidable. On the other hand, we would like to observe that of all the currently known methods of constructing radiation-resistant solar cells, the best is to provide a high level of efficiency for solar cell operation at flux levels of about an order of magnitude above that which is now possible, or in other words, the best we can hope is to improve the efficiency of cell operation about 20 to 30 percent at high flux levels. Thermal annealing is the only method we now know of by which 20 percent damage can be reduced repeatedly to zero.
peatedly to zero.

POSTSCRIPT

Most of the experimental work was completed by the beginning of 1965 and the preparation of this report was started over six months ago. Much more extensive data has been accumulated since that time, but these data are supplementary to that reported here, rather than being of a revisionary nature. Therefore, no efforts were made to alter this report in order to bring it more up to date. Suffice it to say that our original speculative hope that the annealing of radiation damage in solar cells would be possible, seems, on the basis of the data obtained, ever more close to reality.

In the meantime, a phenomenon of mushroom growth – an overnight spreading – has occurred in the study of thermal annealing in semiconductors, both for its intrinsic scientific value and its technical potentialities. If we confine ourselves just to the case of solar cells, we can report that the following laboratories, insofar as our knowledge is complete, are working on the problem:

Hoffman Electronics Corp.	P. Iles
Westinghouse Corp.	J. M. Hicks
NASA Langley Research Center	G. F. Hills
RCA Princeton Laboratories	J. Wysocki

Let us hope that these endeavors will lead to a fruitful solution of an important problem of the space age, in which we have the privilege to live.